Determination of Lu and Hf Mass Fractions and ^{176}Hf/^{177}Hf Ratios in Mafic-Ultramafic Rock Reference Materials by Multi-Collector Inductively Coupled Plasma-Mass Spectrometry

Qian **Ma** (1), Yue-Heng **Yang** (2, 3)* (iD) and Zhi-Ming **Yang** (1) (iD)

(1) Institute of Geology, Chinese Academy of Geological Sciences, Beijing 100037, P.R. China
(2) Institute of Geology and Geophysics, Chinese Academy of Sciences, Beijing 100029, P.R. China
(3) Innovation Academy of Earth Science, Chinese Academy of Sciences, Beijing 100029, P.R. China
* Corresponding author. e-mail: yangyueheng@mail.iggcas.ac.cn

Reported data for Lu, Hf mass fractions and ^{176}Hf/^{177}Hf isotopic ratios of mafic-ultramafic rock reference materials (RMs) are rare at present, hampering the comparison of data quality between difference laboratories. Herein, we measured the Lu and Hf mass fractions and the ^{176}Hf/^{177}Hf isotopic ratios of ten mafic-ultramafic rock RMs, including OKUM (komatiite), WPR-1 (serpentinised peridotite), NIM-N (norite), NIM-P (pyroxenite), UB-N (serpentinised peridotite), JP-1 (peridotite), NIM-D (dunite), MUH-1 (serpentinised harzburgite), HARZ01 (harzburgite), DTS-2b (dunite), which contain extremely low amounts of Lu and Hf (Lu, 2–150 ng g^{-1}; Hf, 5–500 ng g^{-1}). All measurements were conducted on a Neptune Plus multi-collector inductively coupled plasma-mass spectrometer employing an Aridus II desolvator inlet system and Jet sample/X skimmer cone configuration. The following RMs, OKUM, WPR-1, UB-N, JP-1, NIM-D, HARZ01 and DTS-2b, have ^{176}Hf/^{177}Hf precision of less than 60 ppm (2s) at test portions of 0.06 to 0.3 g, and are good ultramafic RMs for Lu-Hf systems. In contrast, significant Hf mass fraction and isotopic variability were observed in NIM-N, NIM-P and MUH-1 at test portion masses of 0.1 to 0.3 g. Collectively, our study provides a new database that can be used by the geochemical community for evaluating the Lu-Hf system of mafic-ultramafic rocks.

Keywords: mafic-ultramafic rock reference materials, bomb and bench-top dissolution, ID-MC-ICP-MS, Lu and Hf mass fractions, ^{176}Hf/^{177}Hf ratio.

The radioactive ^{176}Lu decays by beta emission to stable ^{176}Hf with a decay constant (λ^{176}Lu) of 1.865 $\pm$ 0.015 $\times$ 10^{-11} y^{-1} (Scherer *et al.* 2001), rendering the Lu–Hf isotope system a powerful tool for radiogenic isotopic dating and tracing in cosmochemistry and geochemistry (Blichert-Toft and Albarède 1997a, Blichert-Toft 2001, Barfod *et al.* 2005, Bouvier *et al.* 2015, Vervoort and Kemp 2016, Iizuka *et al.* 2017). The Lu-Hf system is widely used for studying mantle-derived mafic-ultramafic rocks, such as abyssal peridotite, peridotite occurring in ophiolite complexes, and peridotite mantle xenoliths, providing direct information on the chemical components and evolution of mantle–crust systems. (Salters and Zindler 1995, Blichert-Toft and Arndt 1999, Bizimis *et al.* 2007, Salters *et al.* 2011, Mallick *et al.* 2015, Xiong *et al.* 2016, Zhao *et al.* 2021). However, the mass fractions of both Lu and Hf in mafic and ultramafic rocks are generally low (e.g., < 0.5 μg g^{-1}), hindering accurate determination of the Lu and Hf mass fractions and ^{176}Hf/^{177}Hf isotopic ratios.

To achieve reliable measurement of the Lu and Hf mass fractions and ^{176}Hf/^{177}Hf isotopes in highly depleted ultramafic rocks, the following two aspects are required: (1) a high-sensitivity mass spectrometric method to achieve highly precise isotopic measurement results on extremely low amounts of Lu and Hf and (2) a low-blank chemical procedure to completely decompose ultramafic rocks to achieve bias free results. Multi-collector inductively coupled plasma-mass spectrometry (MC-ICP-MS) is widely employed in the determination of ^{176}Hf/^{177}Hf isotopic ratios in geological samples because of its high ionisation efficiency and sample throughput (Blichert-Toft *et al.* 1997b, Halliday

et al. 1998, Münker et al. 2001, Vervoort et al. 2004, Lu et al. 2007, Yang et al. 2010, Bast et al. 2015). It is widely reported that using a dry plasma and a high-efficiency cone configuration could greatly enhance signal sensitivity during MS measurements (e.g., Makishima and Nakamura 2010, Huang et al. 2012). With respect to the sample preparation procedure, HF-assisted digestions (e.g., HF+HNO$_3$, HF+HClO$_4$, or similar mixtures) are commonly used (Ionov et al. 1999, Yang et al. 2010, Ilyinichna et al. 2020). Clean acids can be obtained by repeated sub-boiling distillation, which allows better control of the blank. Earlier studies have widely used two digestion methods for the HF-HNO$_3$ mixture digestion of mafic-ultramafic samples: dissolution in a screw-cap Savillex PFA beaker on a hot plate at 100–120 °C (referred to as "bench-top digestion") and digestion in a high-temperature stainless steel-jacketed polytetrafluoroethylene (PTFE) bomb (Parr or custom-made, referred to as "bomb digestion") at 190–200 °C (Jain et al. 2000, Blichert-Toft et al. 2004, Yang et al. 2010, Li et al. 2014). However, the comparison of the measurement results of these two dissolution methods is not studied for mafic to ultramafic rocks. The resulting insoluble Ca-Mg-fluorides in HF-assisted digestions can be effectively dissolved using saturated boric acid, as boron from the boric acid complexes with free F$^-$, thus releasing Lu and Hf from Ca-Mg fluorides and improving the Lu and Hf recovery yields to > 90 % (e.g., Pin and Santos Zalduegui 1997, Yokoyama et al. 1999, Connelly et al. 2006, Sun et al. 2013, Chu et al. 2014, Frisby et al. 2016, Ma et al. 2019).

Particularly, reference materials (RMs) play an important role in isotopic ratios and elemental mass fractions measurements because RMs are the essential to monitor the quality of data for unknown measurement results and verify the validation of measurement procedures (Weis et al. 2005, Jochum and Nohl 2008, Chauvel et al. 2010, Yang et al. 2020a, Yang et al. 2020b). Using well characterised RMs is particularly important during the Lu-Hf system measurement of mafic-ultramafic plutonic rocks. At present, basaltic RMs are always used as the data quality control materials during measurement of Lu-Hf system in mafic-ultramafic rock samples. However, most plutonic mafic-ultramafic rocks have smaller mass fractions of Lu and Hf (e.g., ≤ 100 ng g^{-1} to several ng g^{-1}) than basalts, and the potential presence of refractory accessory minerals (e.g., spinel, zircon) makes them difficult to be completely dissolved. Thus, using basaltic RMs is not a good idea for quality control as these matrixes have higher Lu and Hf mass fractions compared with mafic-ultramafic rocks and are far easy to digest. It is therefore critical to have homogenous, well characterised matrix-matched mafic-ultramafic rock RMs for method validation and quality control. However,

measurements on the Lu and Hf mass fractions and ^{176}Hf/^{177}Hf isotopic ratios of mafic-ultramafic rock RMs are limited. Currently, most Lu–Hf data on RMs are limited to basaltic samples with high Lu and Hf mass fractions, e.g., BIR-1 (Münker et al. 2001, Bizzarro et al. 2003, Le Fèvre and Pin 2005, Li et al. 2014, Frisby et al. 2016), BCR-1, BCR-2 (Weis et al. 2007), BHVO-1 and BHVO-2 (Weis et al. 2005). Published data on ^{176}Hf/^{177}Hf isotopic ratios in highly depleted rock RMs, such as JP-1, NIM-D, HARZ01, DTS-2b and MUH-1, OKUM, NIM-P, and NIM-N, are limited (Lu et al. 2007, Makishima and Nakamura 2008, 2010, Frisby et al. 2016, Fourny et al. 2016, Ma et al. 2019). To the best of our knowledge, ^{176}Hf/^{177}Hf isotopes in OKUM and WPR-1 are unavailable at present.

In this study, we determined the Lu and Hf mass fractions and ^{176}Hf/^{177}Hf isotopic ratios of ten mafic-ultramafic RMs using MC-ICP-MS and evaluated their suitability as RMs for validation of Lu–Hf system data. The measured RMs include OKUM (Mg-poor komatiite), WPR-1 (serpentinised peridotite), NIM-N (norite), NIM-P (pyroxenite), UB-N (serpentinised peridotite), JP-1 (peridotite), NIM-D (dunite), MUH-1 (serpentinised harzburgite), HARZ01 (harzburgite), DTS-2b (dunite), which contain very low mass fractions of Lu and Hf (Lu, 0.002–0.15 μg g^{-1}; Hf, 0.005–0.5 μg g^{-1}). The measurement results of Lu and Hf mass fractions and ^{176}Hf/^{177}Hf isotopic ratios from bench-top and high-temperature bomb digestions were compared. These results form a new dataset, which is valuable for the isotopic investigation of mafic-ultramafic volcanic and plutonic rocks from a wide range of tectonic settings.

Reference materials

Descriptions of the RMs examined in this study are given in Table 1, including rock type, supplier, locality and relevant major element oxide and Lu, Hf, Zr, Cr mass fractions. Below, detailed information of the key mineralogical and locality geology of the RMs are addressed based on the information provided in the original certificate or reference.

OKUM

The komatiite OKUM is a certified RM issued by the International Association of Geoanalysts (IAG) in 2015. The sample is typical of Mg-poor komatiite or komatiitic basalt; it consists of massive black rocks containing spinifex blades and was collected from a ca. 2.7 Ga spinifex-textured komatiite flow at Serpentine Mountain (McArthur Township) within the Abitibi Greenstone Belt, Ontario, Canada.

Table 1.

Summary of major compositional characteristics and Lu, Hf, Zr, Cr mass fractions of mafic-ultramafic rock RMs in this study

RM	OKUM	WPR-1	NIM-N	NIM-P	UB-N	JP-1	NIM-D	MUH-1	HARZ01	DTS-2b
Rock type	Komatiite	Peridotite	Norite	Pyroxenite	Peridotite	Peridotite	Dunite	Harzburgite	Harzburgite	Dunite
Issuing organisation	IAG	CCRMP	MINTEK	MINTEK	ANRT	GSJ	MINTEK	IAG	IAG	USGS
Locality	Serpentine Mt., McArthur Township, Abitibi Greenstone belt, Ontario, Canada	Wellgreen complex, Yukon, Canada	Main zone of the Bushveld Igneous Complex, South Africa	Critical zone of the Bushveld Igneous Complex, South Africa	Col de Bagenelles (Vosges), France	Horoman peridotite, Horoman, Hokkaido, Japan	Critical zone of the Bushveld Igneous Complex, South Africa	Hartsteinwerke Preg, near Kraubath, Styria, Austria	Devolli, Albania	Twin Sisters Mountain Range, Bellingham, Washington
SiO_2 (% m/m)	44.14	37	52.64	51.1	39.43	42.38	38.96	40.38	43.21	39.4
TiO_2 (% m/m)	0.38	0.30	0.20	0.20	0.11	0.006	0.02	0.0344	-	-
Al_2O_3 (% m/m)	7.97	3.1	16.5	4.18	2.9	0.66	0.30	1.334	0.38	0.45
$Fe_2O_3(T)$ (% m/m)	11.81	14.2	8.97	12.7	8.34	8.37	17.00	8.59	8.952	7.76
MnO (% m/m)	0.1813	0.20	0.18	0.22	0.12	0.121	0.22	0.1179	0.1262	-
MgO (% m/m)	21.29	31	7.5	25.33	35.21	44.6	43.51	38.25	45.84	49.4
CaO (% m/m)	7.85	2.07	11.5	2.66	1.2	0.55	0.28	1.213	0.4781	0.12
Na_2O (% m/m)	1.136	0.041	2.46	0.37	0.1	0.021	0.04	0.104	-	-
Lu (mg kg^{-1})	0.148	0.07	0.09–0.19[a]	0.06–0.07[a]	0.045	0.0044	0.008[b]	0.0191	0.003135	0.0016–0.0037[a]
Hf (mg kg^{-1})	0.551	0.61	0.18–0.6[a]	0.26–0.48[a]	0.1	0.2	0.05[b]	0.044	0.018	0.0029–0.0114[a]
Zr (mg kg^{-1})[a]	14–19	18–22	9–25	7.8–27.4	2.94–5.23	4.02–8.83	1.82[b]	0.66–0.88	-	0.13–0.471
Cr (mg kg^{-1})[a]	2298–2963	3634–3989	18–56.36	23073–25163	1905–2881	1250–3300	-	2561–2960	-	14053–17220

Note: All data are from the issuing organisation, except when noted: [a] GeoReM database (http://georem.mpch-mainz.gwdg.de). [b] Dulski (2001).
IAG: International Association of Geoanalysts; CCRMP: Canadian Certified Reference Materials Project; MINTEK: Council for Mineral Technology; ANRT: Association Nationale de la Recherche Technique; GSJ: Geological Survey of Japan; USGS: United States Geological Survey.

According to Houlé *et al.* (2009), the spinifex texture in the komatiite sills at Serpentine Mountain is mostly composed of olivine and pyroxene crystals. The groundmass occupies approximately 25–35% of the sills and is made up of chlorite, serpentine, devitrified glass, and amphiboles. The olivine blades are tabular, constitute 40–60% of the rock, and are completely replaced by serpentine. Chromium spinel comprises approximately 2–3% of the spinifex-textured sills. Two different habits of chromium spinel are present, dendritic (up to $\sim$ 0.5 mm) and euhedral to subhedral (up to $\sim$0.2 mm), and both are distributed throughout the sills. Both spinel habits are surrounded by thin rims of magnetite.

WPR-1

The peridotite WPR-1 is a certified RM for rare earth and platinum group elements issued by the Canadian Certified Reference Materials Project (CCRMP). The peridotite is from the Wellgreen Complex, Yukon, Canada. It contains antigorite with small amounts of chlorite, accessory magnetite, and chromite, and has the lowest SiO_2 mass fraction (37% m/m) among the RMs in this study (Table 1). The Wellgreen mafic-ultramafic complex is Late Triassic (232.3 $\pm$ 1.0 Ma, zircon U-Pb dating for a Maple Creek gabbro sill, southwest Yukon, Mortensen and Hulbert 1991).

NIM-N

The RM NIM-N (norite) was collected from the Main Zone in the mafic-ultramafic layered rocks (the Rustenburg Layered Suite) of the Bushveld Complex (*ca.* 2.06 Ga, Barnes *et al.* 2010) in the Transvaal, South Africa. Certificate information for major and some trace elements for NIM-N was provided by the Council for Mineral Technology (MINTEK) in 1974. This RM mainly comprises orthopyroxene, plagioclase, magnetite, ilmenite, and clinopyroxene, with minor amounts of quartz and alteration products. The X-ray diffraction analysis confirmed its mineralogical composition (53% labradorite, 24% augite, and 20% enstatite, Fourny *et al.* 2016).

NIM-P

The NIM-P is a pyroxenite that has been certified for its major and some trace elements, issued by MINTEK in 1974. The sample was collected from the Critical Zone in the ultramafic to mafic layered rocks (the Rustenburg Layered Suite) of the Bushveld Complex in Transvaal, South Africa. It consists of orthopyroxene, clinopyroxene, and plagioclase with minor amounts of olivine and chromite. The Critical Zone is host to cyclic units of chromitites, pyroxenites, and norites (Barnes *et al.* 2010).

UB-N

The reference material UB-N was prepared by the Association Nationale de la Recherche Technique (ANRT) and was first distributed as a powdered reference material in 1967 (Govindaraju 1982). It is a serpentinised garnet and spinel-bearing peridotite (a metamorphosed lherzolite) sampled from the Vosges Mountains, France. The sample is well characterised for mineral chemistry, major elements, many trace elements, and Re-Os systematics (Meisel *et al.* 2003). Details on the chemical composition and ordering information can be found at https://sarm.cnrs.fr/pages/details.php?standard=UB-N. According to the certificate, a working value of 0.045 ± 0.005 µg g^{-1} (95% confidence, $n = 10$) and a proposed value of 0.1 µg g^{-1} are assigned to the Lu and Hf mass fractions, respectively.

JP-1

The peridotite reference material JP-1 was collected by the Geological Survey of Japan (GSJ) from the Horoman Peridotite Complex, Hokkaido, Japan. The Horoman massif is a well-preserved, non-serpentinised orogenic peridotite complex exposed at the southern end of the Hidaka metamorphic belt (Anguelova *et al.* 2022). The specific mineral composition of JP-1 is unknown. Details on the major, minor, and trace elements in JP-1 can be found at https://gbank.gsj.jp/geostandards/igneous.html.

NIM-D

The reference material NIM-D is a dunite from an ultrabasic pipe that crosses the Critical Zone of the Bushveld Complex in South Africa prepared by MINTEK in 1974. It consists of olivine and orthopyroxene with minor amounts of clinopyroxene, plagioclase, and chromite.

MUH-1

The harzburgite MUH-1 is a RM certified for major and trace elements according to ISO Guides 34 and 35, issued by the IAG in 2015. Details on the chemical composition and ordering information can be found at http://iageo.com/muh-1-harzburgit-kraubath/. This reference material was collected from the "Hartsteinwerke Preg" quarry near Kraubath, Styria, Austria. The Kraubath massif consists of layered dunite, harzburgite and bronzitite, which forms part of the Spike Complex and represents the largest outcrop of ultramafic rocks in the Eastern Alps. The mafic and ultramafic from Kraubath Massif have been described as remnants of oceanic crust that formed during the Palaeozoic (Meisel *et al.* 1997, Melcher and Meisel 2004). The MUH-1 reference material consists of partially serpentinised harzburgite with an approximate volumetric mineral composition of 57% serpentine, 35% olivine, 5% brucite, traces (0.2–1%) of calcic amphibole, magnetite, talc, chromite, and enstatite, and ultra-traces ($< 0.01\%$) of Fe-Ni sulfide.

HARZ01

The HARZ01 (harzburgite) was produced from 100 kg of unserpentinised harzburgite collected from the Devolli Gorge, Southeast Albania. Certificate information for major and trace elements for this RM was derived from the proficiency testing programme GeoPT (round 38A), which was directed by the IAG (Webb *et al.* 2016). This material is highly depleted in many lithophile trace elements, which has led to challenges in accurate analysis for many laboratories. The indicative value for Hf mass fraction was 0.018 µg g^{-1}, which was achieved by laboratories employing ICP-MS using acid digestion.

DTS-2b

The DTS-2b is a dunite collected from a quarry located in the Twin Sisters Range, Washington, the same general location as DTS-1. The ultramafic massif forming the Twin Sisters Range is largely comprises unserpentinised dunite and harzburgite with Cr-spinel, minor clinopyroxene, and rare amphibole (Ragan 1963, Toy *et al.* 2010). Certificate information (not according to ISO Guides) for major and some trace elements for DTS-2b was provided by the United States Geological Survey (USGS). According to the certificate, DTS-2 consists of forsterite ($> 90\%$) with minor amounts of chromite and trace amounts of lizardite.

Measurement procedures

Laboratory environment, reagents and materials

Digestion and separation were carried out in class 100 fume hoods located in a class 1000 clean laboratory at the State Key Laboratory of Lithospheric Evolution, Institute of Geology and Geophysics (IGG), Chinese Academy of Sciences (CAS), Beijing. De-ionised water (18.2 $M\Omega$ cm resistivity, Elix-Millipore, USA) was used throughout. Concentrated HCl, HNO_3, and HF (trace metal grade, Beijing Institute of Chemical Reagents) were further purified by a Savillex DST-1000 sub-boiling distillation system (Minnetonka, MN, USA). Additionally, $HClO_4$ (Sigma-Aldrich, MO, USA, weight percent = 70%), H_3BO_3 (powder, trace metal grade, Acros, Geel, Belgium, 99.99% purity), and H_2O_2 (Beijing Institute of Chemical Reagents, w = 30%) were used as received. Sample digestions were performed in 15 ml Savillex PFA vials or 15 ml custom-made PTFE bombs. These vials and bombs were thoroughly cleaned using a multi-step procedure: (1) batch cleaning in 50% v/v HCl solution (trace metal grade), (2) batch cleaning in 50% v/v HNO_3 solution (trace metal grade), (3) fluxing closed in 6 mol l^{-1} HCl solution (further purified by a Savillex DST-1000 sub-boiling distillation system), and (4) fluxing closed in 7 mol l^{-1} HNO_3 solution (further purified by a Savillex DST-1000 sub-boiling distillation system). Each of these steps was performed for a minimum of 24 h on a hot plate at 100 °C, rinsing several times with 18.2 $M\Omega$ cm water between each step. Steps (3) and (4) were found to be critical for reproducible low Hf blanks.

Lutetium and Hf tracers (spikes with enriched ^{176}Lu-^{180}Hf isotopes) were purchased from Oak Ridge National Laboratory, USA, the solutions were calibrated by reverse isotope dilution (ID) against gravimetric standards (Yang et al. 2010). The standard solutions of JMC475 Hf provided by P.J. Patchett and Alfa Hf (Stock no. 14374) purchased from Alfa Aesar (USA) were gravimetrically diluted with 2% v/v HNO_3 + 0.1% v/v HF to 20 ng g^{-1} of Hf solution for mass spectrometric measurements.

Sample preparation and column chemistry

Replicates (n = 2–8) of each RM as sent by the issuing organisation (without additional drying) were measured in this study. Approximately 60–300 mg of rock powder (powders of each material were from the same vial) and ^{176}Lu-^{180}Hf mixed spike were weighed (both to 0.01 mg precision) and digested using an acid mixture of 2 ml

22 mol l^{-1} HF, 1 ml 14 mol l^{-1} HNO_3, and 0.2 ml $HClO_4$ (weight percent = 70%) either using bench-top or bomb digestion for one week (Yang et al. 2010). For sample size > 200 mg, 4 ml 22 mol l^{-1} HF, 2 ml 14 mol l^{-1} HNO_3, and 0.4 ml $HClO_4$ (weight percent = 70%) were used. When using bombs, rock samples and spikes were weighted and digested directly in contact with the PFA vials. After cooling, the beakers and bombs were opened and heated at 190 °C until they were dried, and the solution was evaporated to dryness to remove HF. Then, 3 ml of 6 mol l^{-1} HCl was added to the residue and allowed to dry at 100 °C; this procedure was repeated twice. The residues were dissolved in 3–5 ml saturated solution (~ 0.45 mol l^{-1}) of boric acid in 3 mol l^{-1} HCl (corresponding to 0.028 g boric acid crystals per ml of 3 mol l^{-1} HCl) at 100 °C on a hot plate overnight before being dried down and re-dissolved in 3–5 ml saturated solution of boric acid; by then, the sample was ready for column chemistry. The amount of boric acid solution used was in proportion to the sample mass, i.e., 3 ml boric acid in 3 mol l^{-1} HCl was used for sample masses < 200 mg and 5 ml boric acid in 3 mol l^{-1} HCl was used for sample masses > 200 mg. The signal intensity of ^{177}Hf for JP-1 peridotite was 0.02 V and approximately 1 V before and after H_3BO_3 treatment, demonstrating the effective decomposition of fluoride during sample digestion. Using saturated H_3BO_3 in 3 mol l^{-1} HCl in the final dissolution procedure, highly clear residue-free sample solutions were obtained.

The sample solution was centrifuged and then loaded onto 2 ml pre-conditioned Ln Spec resin to separate of Lu and Hf from the sample matrix (Münker et al. 2001, Yang et al. 2010). A detailed description of the column chemistry can be found in Ma et al. (2019) and the following is a brief introduction. Matrix elements (including major and light rare earth elements) were eluted with 3 mol l^{-1} and 4 mol l^{-1} HCl. The Lu (+Yb) fraction was eluted subsequently with 4 mol l^{-1} HCl, evaporated to dryness, and diluted to 1 ml with 2% v/v HNO_3 prior to mass spectrometry. To maximise the separation between Hf and the heavy rare earth elements, the column was rinsed with 40 ml of 6 mol l^{-1} HCl to effectively remove Lu and Yb residues. Subsequently, titanium was separated from Hf by rinsing the column with a 20 ml 4 mol l^{-1} HCl + 0.5% v/v H_2O_2 mixture. Finally, Hf-Zr factions were extracted from the column with 5 ml of 2 mol l^{-1} HF, collected in a 7-ml PFA beaker, and evaporated to dryness at 80 °C on a hot plate. This fraction was taken in 0.01 ml 2 mol l^{-1} HF, diluted to 1 ml with 2% v/v HNO_3, and was then ready for Hf isotopic measurement. The recovery yields of Lu and Hf were higher than 50% and 90%, respectively. The total procedure blanks for Lu and Hf were mostly lower than 5 pg and 10 pg, respectively, using bench-top digestion.

Mass spectrometry

Isotopic compositions were measured using a Thermo Fisher Scientific Neptune Plus MC-ICP-MS (Bremen, Germany), housed at IGG, CAS, and equipped with nine Faraday cups with 10^{11} ohm resistor pre-amplifiers. The Lu–Hf isotopic data were acquired in multi-collector modes with low resolution. The Neptune Plus cup configurations for Lu measurement were $^{168}Er+Yb^+$ on L4, $^{170}Er+Yb^+$ on L3, $^{171}Yb^+$ on L2, $^{172}Yb^+$ on L1, $^{173}Yb^+$ on the centre cup, $^{174}Yb+Hf^+$ on H1, $^{175}Lu^+$ on H2, $^{176}Lu+Yb+Hf^+$ on H3, and $^{178}Hf^+$ on H4. For Hf measurement, the cup configurations were $^{173}Yb^+$ on L4, $^{175}Lu^+$ on L3, $^{176}Hf+Yb+Lu^+$ on L2, $^{177}Hf^+$ on L1, $^{178}Hf^+$ on the centre cup, $^{179}Hf^+$ on H1, $^{180}Hf+Ta+W^+$ on H2, $^{181}Ta^+$ on H3, and $^{186}W^+$ on H4. The sample solution was introduced with a CETAC Aridus II desolvator using a Savillex C-flow 50 ml min^{-1} high-temperature-resistant (110 °C) nebuliser. The cone configuration was the Jet sample/X skimmer cone. With this high-sensitivity dry plasma analysis and high-efficiency cone configuration, the Hf sensitivity was approximately 10–15 times higher than that of the solution inlet system. A 20 ng g^{-1} Alfa Hf or JMC475 Hf standard solution was used to optimise the instrumental parameters to achieve the highest sensitivity while maintaining low oxide concentration ($HfO^+/Hf^+ < 0.2\%$), flat-top peaks, and stable signals and to evaluate the stability of the instrument. Normally, a 4–5 V signal intensity was obtained for ^{180}Hf in a 20 ng g^{-1} Hf standard solution, assuming that the sample gas and ion beam were carefully optimised. A 2% v/v HNO$_3$ + 0.1% v/v HF solution was used as both the carrier and the washing solution.

Each measurement consisted of nine blocks with nine cycles per block. The integration time was 8 s per cycle. The raw data were reduced offline to correct for instrumental mass bias and spike contribution, followed by normalisation to $^{179}Hf/^{177}Hf = 0.7325$ using the exponential law. The Lu measurement consisted of one block of forty cycles with an integration time of 4 s. The mass bias behaviour of Lu was assumed to follow that of Yb for the interference correction of ^{176}Yb on ^{176}Lu using the exponential law ($^{176}Yb/^{172}Yb = 0.588673$ and $^{173}Yb/^{172}Yb = 0.739251$, Vervoort et $al.$ 2004). The Lu mass fraction of the sample was calculated from the corrected $^{176}Lu/^{175}Lu$ ratios using the isotope dilution equation. The data reduction was performed by a computer using a self-written Excel VBA (Visual Basic for Applications) macro program, within which interference corrections and spike subtractions are made.

Results and discussion

The Lu and Hf mass fractions, and $^{176}Hf/^{177}Hf$ isotopic ratios and corresponding test portion size for the RMs measured in this study are presented in Table 2, where each line represents the separate digestion of different powder aliquots. The measured data of each RM were also compared with available data of independent labs reported in the literature (Table 3, Figure 4). For the final Lu, Hf mass fractions and $^{176}Hf/^{177}Hf$ ratio data set for each RM, the standard deviation at the 95% confidence level (2s) of the mean is given as an estimate of data intermediate precision.

Measurement results of Hf standard solution

The standard solutions JMC 475 Hf and Alfa Hf were repeatedly measured during different measurement sessions over four years (Figure 1). The mean $^{176}Hf/^{177}Hf$ ratio of the measured 10 ng g^{-1} JMC475 Hf standard solution (10 ng Hf) was 0.282160 ± 0.000016 (2s, $n = 74$), which was in excellent agreement with previously reported values (0.282160, Weis et $al.$ 2007). The mean $^{176}Hf/^{177}Hf$ ratio of the 20 ng g^{-1} Alfa Hf standard solution (20 ng Hf) was 0.282186 ± 0.000012 (2s, $n = 108$). These results are in excellent agreement with those previously obtained using an MC-ICP-MS with a wet-method spray chamber and PFA self-aspirating nebuliser (> 100 ng Hf) (Yang et $al.$ 2010), indicating the insignificant bias for the standard solution measurement with the instrumental method used. The internal precision of the $^{176}Hf/^{177}Hf$ ratio was better than 20 ppm (2SE) for 10 ng Hf and better than 10 ppm (2SE) for 20 ng Hf. The standard deviation at the 95% confidence level (2s) is given as an estimate of data intermediate precision of Hf standard solution. The intermediate precision of the results of 10 ng g^{-1} JMC475 Hf and 20 ng g^{-1} Alfa Hf standard solution were better than 16 and 12 ppm, respectively, demonstrating the long-term stability of the instrumental method.

Mafic-ultramafic RMs with Hf mass fraction of 100–500 ng g^{-1}

The OKUM has the highest Lu and Hf mass fractions among the mafic-ultramafic rock RMs in this study. As shown in Table 2, the mean values of Lu and Hf mass fractions obtained using the bomb digestion method for OKUM were 149 ± 2 ng g^{-1} (2s, n = 5) and 564 ± 19 ng g^{-1} (2s, n = 5), respectively, whereas the bench-top solution yielded identical Lu mass fractions (147 ± 6 ng g^{-1}, 2s, n = 4) and

Table 2.
Measurement results of Lu and Hf mass fraction and $^{176}Hf/^{177}Hf$ isotopic ratio of mafic–ultramafic rock RMs in this study

RM (Rock type) (test portion size)	Lu (ng g⁻¹)	Hf (ng g⁻¹)	$^{176}Lu/^{177}Hf$	$^{176}Hf/^{177}Hf$ ($\pm$2SE)	Dissolution method[d]	Analysis date
OKUM (Mg-poor komatiite, 60 mg, ^{177}Hf signal intensity: ~ 2.5 V)						
				0.283282(07)*	Bench-top	11/12/2017
				0.283286(07)*	Bench-top	11/12/2017
	146	515	0.0402	0.283289(11)	Bench-top	09/18/2017
	146	525	0.0396	0.283247(10)	Bench-top	09/18/2017
	145	510	0.0403	0.283269(07)	Bench-top	11/12/2017
	141	505	0.0397	0.283289(07)	Bench-top	11/12/2017
Mean [$\pm$2s][a]	144[5]	514[17]	0.0399[07]	0.283273[40]	Bench-top	
	148	555	0.0379	0.283157(12)	Bomb	12/04/2018
	148	554	0.0380	0.283150(11)	Bomb	12/04/2018
	150	576	0.0370	0.283138(10)	Bomb	03/05/2019
	150	568	0.0376	0.283169(12)	Bomb	03/05/2019
	149	568	0.0373	0.283150(10)	Bomb	03/05/2019
Mean [$\pm$2s][b]	**149[2]**	**564[19]**	**0.0375[08]**	**0.283153[23]**	**Bomb (preferred)**	
Mean [$\pm$2s][a+b]	147[6]	542[56]	0.0386[26]	0.283206[131]		
WPR-1 (serpentinised peridotite, 60 mg, ^{177}Hf signal intensity: ~ 2.5 V)						
				0.282974(08)*	Bench-top	09/27/2018
				0.282970(07)*	Bench-top	09/27/2018
	65.1	504	0.0184	0.282973(08)	Bench-top	09/27/2018
	63.8	504	0.0180	0.282975(14)	Bench-top	09/27/2018
	62.5	483	0.0184	0.282983(08)	Bench-top	09/27/2018
	63.5	508	0.0178	0.282977(08)	Bench-top	09/27/2018
	64.0	515	0.0177	0.282970(07)	Bench-top	03/05/2019
	63.1	504	0.0178	0.282997(06)	Bench-top	03/05/2019
	62.9	525	0.0170	0.282977(08)	Bench-top	03/05/2019
Mean [$\pm$2s][a]	63.6[1.7]	506[26]	0.0179[10]	0.282979[18]	Bench-top	
				0.282941(12)*	Bomb	12/04/2018
	62.9	518	0.0173	0.282949(10)	Bomb	12/04/2018
	62.6	542	0.0164	0.282954(13)	Bomb	12/04/2018
	63.3	540	0.0167	0.282971(06)	Bomb	03/05/2019
	61.7	538	0.0163	0.282967(06)	Bomb	03/05/2019
	62.6	532	0.0167	0.282960(06)	Bomb	03/05/2019
Mean [$\pm$2s][b]	**62.6[1.2]**	**532[20]**	**0.0167[08]**	**0.282960[18]**	**Bomb (preferred)**	
Mean [$\pm$2s][a+b]	63.2[1.7]	518[36]	0.0174[15]	0.282970[28]		
NIM-N (norite, 100 mg, ^{177}Hf signal intensity: ~ 2.5 V)						
				0.282878(08)*	Bench-top	11/12/2017
				0.282855(08)*	Bench-top	11/12/2017
	103	349	0.0417	0.282870(09)	Bench-top	09/18/2017
	102	369	0.0393	0.282763(06)	Bench-top	11/12/2017
	102	351	0.0413	0.282843(06)	Bench-top	11/12/2017
Mean [$\pm$2s][a]	102[1]	356[22]	0.0408[25]	0.282825[111]	Bench-top	
				0.282883(09)*	Bomb	12/04/2018
				0.282869(10)*	Bomb	12/04/2018
				0.282860(09)*	Bomb	12/042018
	104	346	0.0425	0.282905(08)	Bomb	12/04/2018
	104	345	0.0428	0.282905(08)	Bomb	12/04/2018
	104	345	0.0428	0.282907(12)	Bomb	12/04/2018
	103	348	0.0421	0.282885(12)	Bomb	12/04/2018
	103	350	0.0420	0.282917(06)	Bomb	03/05/2019
	105	355	0.0421	0.282900(05)	Bomb	03/05/2019
	104	352	0.0420	0.282890(06)	Bomb	03/05/2019
	104	350	0.0424	0.282912(06)	Bomb	03/05/2019
Mean [$\pm$2s][b]	104[1]	349[7]	0.0423[07]	0.282903[21]	Bomb	
Mean [$\pm$2s][a+b]	103[2]	351[13]	0.0419[19]	0.282878[38]		

Table 2 (continued).
Measurement results of Lu and Hf mass fraction and ^{176}Hf/^{177}Hf isotopic ratio of mafic-ultramafic rock RMs in this study

RM (Rock type) (test portion size)	Lu (ng g^{-1})	Hf (ng g^{-1})	^{176}Lu/^{177}Hf	^{176}Hf/^{177}Hf ($\pm$2SE)	Dissolution method[d]	Analysis date
NIM-P (pyroxenite, 100 mg, ^{177}Hf signal intensity: ~ 2 V)						
				0.282496(08)*	Bench-top	11/12/2017
				0.282760(08)*	Bench-top	11/12/2017
	64.0	259	0.0351	0.282670(09)	Bench-top	09/18/2017
	64.0	295	0.0308	0.282477(08)	Bench-top	09/18/2017
	63.5	243	0.0372	0.282765(08)	Bench-top	11/12/2017
	63.6	266	0.0339	0.282618(07)	Bench-top	11/12/2017
Mean [$\pm$2s][a]	63.8[0.5]	266[44]	0.0343[53]	0.282633[240]	Bench-top	
	64.8	319	0.0289	0.282408(08)	Bomb	12/04/2018
	64.7	273	0.0337	0.282610(11)	Bomb	12/04/2018
	64.3	276	0.0331	0.282575(17)	Bomb	12/04/2018
	64.2	299	0.0305	0.282482(09)	Bomb	12/04/2018
				0.282472(09)*	Bomb	12/04/2018
				0.282393(08)*	Bomb	12/04/2018
				0.282731(14)*	Bomb	12/04/2018
	64.2	274	0.0333	0.282603(05)	Bomb	03/05/2019
	64.4	262	0.0349	0.282659(07)	Bomb	03/05/2019
	63.3	266	0.0338	0.282631(06)	Bomb	03/05/2019
	62.4	278	0.0319	0.282546(07)	Bomb	03/05/2019
Mean [$\pm$2s][b]	64.0[1.6]	281[38]	0.0325[39]	0.282564[167]	Bomb	
Mean [$\pm$2s][a+b]	64.0[1.3]	276[41]	0.0331[39]	0.282582[231]		
UB-N (serpentinised peridotite, 150 mg, ^{177}Hf signal intensity: ~ 1.5 V)						
				0.283272(09)*	Bench-top	08/01/2018
				0.283265(09)*	Bench-top	08/01/2018
				0.283248(08)*	Bench-top	08/01/2018
	43.9	127	0.0492	0.283275(17)	Bench-top	07/26/2018
	43.9	127	0.0492	0.283256(12)	Bench-top	07/26/2018
	44.4	125	0.0505	0.283255(07)	Bench-top	08/01/2018
	44.6	125	0.0506	0.283239(10)	Bench-top	08/01/2018
Mean [$\pm$2s][a]	44.2[0.7]	126[2]	0.0499[16]	0.283256[29]	Bench-top	
	45.8	128	0.0510	0.283272(20)	Bomb	12/04/2018
	45.5	134	0.0483	0.283229(19)	Bomb	12/04/2018
	45.1	121	0.0528	0.283295(07)	Bomb	03/05/2019
	46.1	127	0.0516	0.283268(05)	Bomb	03/05/2019
	45.8	123	0.0530	0.283302(06)	Bomb	03/05/2019
	45.6	120	0.0539	0.283305(08)	Bomb	03/05/2019
Mean [$\pm$2s][b]	45.7[0.7]	125[10]	0.0518[40]	0.283273[51]	Bomb	
Mean [$\pm$2s][a+b]	**45.1[1.6]**	**126[8]**	**0.0510[37]**	**0.283268[46]**	**Bench-top/Bomb (preferred)**	
JP-1 (peridotite, 150 mg, ^{177}Hf signal intensity: ~ 1 V)						
				0.282301(10)*	Bench-top	12/07/2016
	3.97	121	0.00467	0.282293(08)	Bench-top	12/07/2016
	4.03	117	0.00491	0.282325(07)	Bench-top	12/07/2016
	3.97	118	0.00479	0.282293(08)	Bench-top	12/07/2016
				0.282300(10)*	Bench-top	09/18/2017
	4.06	118	0.00488	0.282307(07)	Bench-top	09/18/2017
	4.12	119	0.00492	0.282298(07)	Bench-top	09/18/2017
				0.282303(07)*	Bench-top	01/31/2018
	3.88	116	0.00474	0.282301(09)	Bench-top	01/31/2018
	3.93	116	0.00483	0.282293(08)	Bench-top	01/31/2018
Mean [$\pm$2s][a]	3.99[0.16]	118[4]	0.00482[19]	0.282301[23]	Bench-top	
				0.282307(17)*	Bomb	12/04/2018
				0.282316(06)*	Bomb	12/04/2018
	3.99	118	0.00479	0.282329(17)	Bomb	12/04/2018
	4.23	119	0.00504	0.282317(07)	Bomb	12/04/2018
Mean [$\pm$2s][b]	4.11[0.34]	119[1]	0.00492[35]	0.282323[17]	Bomb	
Mean [$\pm$2s][a+b]	**4.02[0.21]**	**118[3]**	**0.00484[21]**	**0.282306[22]**	**Bench-top/Bomb (preferred)**	

Table 2 (continued).
Measurement results of Lu and Hf mass fraction and $^{176}Hf/^{177}Hf$ isotopic ratio of mafic-ultramafic rock RMs in this study

RM (Rock type) (test portion size)	Lu (ng g^{-1})	Hf (ng g^{-1})	$^{176}Lu/^{177}Hf$	$^{176}Hf/^{177}Hf$ ($\pm$2SE)	Dissolution method[d]	Analysis date
NIM-D (dunite, 300 mg, ^{177}Hf signal intensity: ~ 1 V)						
	8.30	56.6	0.0209	0.282728(10)*	Bench-top	07/26/2018
	8.35	57.1	0.0208	0.282766(09)	Bench-top	07/26/2018
	8.89	55.9	0.0226	0.282743(09)	Bench-top	07/26/2018
Mean [$\pm$2s][a]	8.51[0.65]	56.5[1.2]	0.0214[20]	0.282730(13)	Bench-top	03/05/2019
				0.282746[36]	Bench-top	
				0.282692(10)*	Bomb	03/05/2019
	7.98	56.7	0.0200	0.282696(09)	Bomb	03/05/2019
	8.20	57.2	0.0203	0.282707(11)	Bomb	03/05/2019
	7.07	45.6	0.0220	0.282762(09)	Bomb	03/05/2019
	8.56	55.0	0.0221	0.282742(10)	Bomb	03/05/2019
Mean [$\pm$2s][b]	7.95[1.27]	53.6[10.9]	0.0211[22]	0.282727[61]	Bomb	
Mean [$\pm$2s][a+b]	**8.19[1.14]**	**54.9[8.3]**	**0.0212[20]**	**0.282730[54]**	**Bench-top/Bomb (preferred)**	
MUH-1 (serpentinised harzburgite, 300 mg, ^{177}Hf signal intensity: ~ 0.5 V)						
	17.1	27.3	0.0891	0.283568(12)	Bench-top	07/26/2018
	17.8	27.3	0.0926	0.283635(13)	Bench-top	08/01/2018
				0.283559(12)*	Bench-top	09/28/2018
	18.0	29.8	0.0857	0.283575(10)	Bench-top	09/28/2018
	18.7	26.5	0.1003	0.283661(08)	Bench-top	03/05/2019
Mean [$\pm$2s][a]	17.9[1.3]	27.7[2.9]	0.0919[125]	0.283610[91]	Bench-top	
				0.283551(12)*	Bomb	03/05/2019
	18.2	41.2	0.0626	0.283351(08)	Bomb	03/05/2019
	18.2	39.5	0.0656	0.283419(08)	Bomb	03/05/2019
	18.1	31.8	0.0809	0.283533(09)	Bomb	03/05/2019
	17.3	46.6	0.0527	0.283293(10)	Bomb	03/05/2019
Mean [$\pm$2s][b]	18.0[0.9]	39.8[12.2]	0.0655[234]	0.283399[206]	Bomb	
Mean [$\pm$2s][a+b]	17.9[1.0]	33.8[5.3]	0.0787[332]	0.283515[241]		
HARZ01 (harzburgite, 300 mg, ^{177}Hf signal intensity: ~ 0.3 V)						
				0.282348(14)*	Bench-top	09/28/2018
	3.03	13.8	0.0312	0.282377(12)	Bench-top	03/05/2019
	3.04	14.3	0.0302	0.282365(14)	Bench-top	03/05/2019
	3.07	15.7	0.0278	0.282353(13)	Bench-top	03/05/2019
Mean [$\pm$2s][a]	3.05[0.04]	14.6[2.0]	0.0297[35]	0.282365[24]	Bench-top	
				0.282370(18)*	Bomb	03/05/2019
	2.85	13.2	0.0306	0.282417(13)	Bomb	03/05/2019
	2.74	16.7	0.0234	0.282366(10)	Bomb	03/05/2019
	2.83	13.8	0.0291	0.282342(16)	Bomb	03/05/2019
	2.86	13.9	0.0294	0.282378(23)	Bomb	03/05/2019
Mean [$\pm$2s][b]	2.82[0.11]	14.4[3.1]	0.0281[64]	0.282376[63]	Bomb	
Mean [$\pm$2s][a+b]	**2.82[0.26]**	**14.5[2.5]**	**0.0288[53]**	**0.282368[44]**	**Bench-top/Bomb (preferred)**	
DTS-2b (dunite, 300 mg, ^{177}Hf signal intensity: ~ 0.15 V)						
	1.70	3.76	0.0641	0.283088(51)	Bench-top	07/26/2018
	2.15	4.31	0.0708	0.283092(20)	Bench-top	03/05/2019
	1.95	4.46	0.0622	0.283094(29)	Bench-top	03/05/2019
				0.283080(29)*	Bench-top	06/26/2018
Mean [$\pm$2s][a]	1.93[0.45]	4.18[0.74]	0.0657[90]	0.283091[06]	Bench-top	
	2.12	4.48	0.0671	0.283076(37)	Bomb	03/05/2019
	2.02	4.40	0.0653	0.283076(56)	Bomb	03/05/2019
				0.283069(24)*	Bomb	03/05/2019
				0.283091(42)*	Bomb	03/05/2019
	2.09	4.57	0.0648	0.283051(62)	Bomb	03/05/2019
Mean [$\pm$2s][b]	2.08[0.10]	4.48[0.17]	0.0657[24]	0.283068[29]	Bomb	

Table 2 (continued).

Measurement results of Lu and Hf mass fraction and ^{176}Hf/^{177}Hf isotopic ratio of mafic–ultramafic rock RMs in this study

RM (Rock type) (test portion size)	Lu (ng g^{-1})	Hf (ng g^{-1})	^{176}Lu/^{177}Hf	^{176}Hf/^{177}Hf ($\pm$2SE)	Dissolution method[d]	Analysis date
Mean [$\pm$2s][a+b]	2.01[0.17]	4.33[0.22]	0.0657[59]	0.283081[26]	Bench-top/Bomb (preferred)	

Note: [a] The mean values were calculated based on the isotope-dilution (ID) method using bench-top digestion.

[b] The mean values were calculated based on the ID method using bomb digestion.

[a+b] The mean values were calculated based on the ID method using bench-top digestion and bomb digestion.

The ^{176}Hf/^{177}Hf values were determined from spiked sample analyses, except for those marked with an asterisk (*), which were determined from unspiked analyses.

$\pm$2SE, 2 standard error ("internal precision"); $\pm$2s, two standard deviations (intermediate precision) based on multiple analyses and are reported as times 10^6 for ^{176}Hf/^{177}Hf ratios and 10^4 for ^{176}Lu/^{177}Hf, except 10^5 for ^{176}Lu/^{177}Hf of JP-1.

lower Hf mass fractions (514 ± 17 ng g^{-1}, 2s, n = 4). Data of OKUM from the two dissolution methods lie on an approximately 2.7 Ga reference line (Figure 2a). The values obtained with bomb dissolution offer good intermediate precision (Rs < 3%) and are in excellent agreement with the IAG-certified values and previously determined values by ICP-MS (Table 3 and Figure 4; Waterton et al. 2016, Locmelis et al. 2016) and LA-ICP-MS (Peters and Pettke 2017, Gilio et al. 2019). With bomb dissolution, the corresponding mean ^{176}Lu/^{177}Hf is 0.0375 ± 0.0008 (2s, n = 5), and all ^{176}Hf/^{177}Hf isotopic ratio (spiked and non-spiked) gave a mean of ^{176}Hf/^{177}Hf = 0.283153 ± 0.000023 (2s, n = 5).

For WPR-1, the mean values of Lu and Hf mass fractions using two digestion methods were 63.2 ± 1.7 ng g^{-1} (2s, n = 12) and 518 ± 36 ng g^{-1} (2s, n = 12), respectively. The corresponding mean ^{176}Lu/^{177}Hf was 0.0174 ± 0.0015 (2s, n = 12), and all ^{176}Hf/^{177}Hf isotopic ratio (spiked and non-spiked) yielded a mean of ^{176}Hf/^{177}Hf = 0.282970 ± 0.000028 (2s, n = 15). The ^{176}Hf/^{177}Hf isotopic ratio for the two dissolution methods was relatively reproducible with intermediate precision better than 30 ppm (2s). Both Lu and Hf mass fractions obtained in this study were approximately 10% lower than the provisional values from CCRMP and one value measured on ICP-MS by Chu et al. (2009). As the Lu and Hf mass fractions were measured using the isotope dilution technique in this study, we believe that our values were probably less biased. To the best of our knowledge, we are the first to publish the ^{176}Hf/^{177}Hf isotopic data for OKUM and WPR-1.

The RMs NIM-N and NIM-P were both collected from the Bushveld Complex in South Africa, and the Lu-Hf data are laid on a line with a slope consistent with an age of 2.0 Ga (Figure 2c, d), similar to the published ages of the intrusion of mafic-ultramafic rocks from the Bushveld Complex (2.05 Ga, Scoates and Friedman 2008). In

this study, the mean values and their intermediate precision of Lu and Hf mass fractions of NIM-N using the two dissolution methods was 103 ± 2 ng g^{-1} (2s, n = 11) and 351 ± 13 ng g^{-1} (2s, n = 11), respectively. The values are identical to that reported by Dulski (2001), who determined it by bomb digestion and ICP-MS. The corresponding mean ^{176}Lu/^{177}Hf ratio was 0.0419 ± 0.0019 (2s, n = 11) and mean ^{176}Hf/^{177}Hf ratios for two dissolution methods was 0.282878 ± 0.000038 (2s, n = 16), which agrees well with the previous 0.282824 ± 0.000110 (2s, n = 10) reported by Fourny et al. (2016).

Using bench-top and bomb digestion procedures, the mean Lu mass fractions of NIM-P was 64.0 ± 1.3 ng g^{-1} (2s, n = 12), whereas the Hf mass fractions and ^{176}Hf/^{177}Hf isotopic ratios were relatively variable. The previously reported Hf isotopic data measured on a Nu Instrument MC-ICP-MS by Fourny et al. (2016) was 0.282484 ± 0.000072 (2s, n = 3). In this study, the Hf mass fractions ranged from 243 ng g^{-1} to 319 ng g^{-1}, and the ^{176}Hf/^{177}Hf ratios ranged from 0.282393 to 0.282765, indicating the heterogeneity in Hf mass fractions and ^{176}Hf/^{177}Hf of NIM-P.

Here, using bomb and bench-top digestion, UB-N yielded mean Lu and Hf mass fractions of 45.1 ± 1.6 ng g^{-1} (2s, n = 10) and 126 ± 8 ng g^{-1} (2s, n = 10), respectively, which were consistent with previous values obtained using ICP-MS (Deschamps et al. 2010, Chauvel et al. 2011, Rospabé et al. 2018, Debret et al. 2019) and LA-ICP-MS (bulk rock pressed powder pellets, Peters and Pettke 2017). The corresponding mean ^{176}Lu/^{177}Hf ratio was 0.0510 ± 0.0037 (2s, n = 10), and all ^{176}Hf/^{177}Hf isotopic data (spiked and non-spiked) yielded a calculated mean of 0. 283268 ± 0.000046 (2s, n = 13). These values were identical to our previously reported values (Lu = 45.5 ± 0.4 ng g^{-1}, Hf = 125.5 ± 3.0 ng g^{-1}, ^{176}Lu/^{177}Hf = 0.0516 ± 0.0008, ^{176}Hf/^{177}Hf = 0.283245 ± 0.000011, 2s, n = 3; Ma et al. 2019).

Table 3.
Comparison of Lu and Hf mass fractions, and $^{176}Hf/^{177}Hf$ isotope ratios obtained in this study with published values for mafic–ultramafic rock RMs

RM	Lu (±2s) (ng g⁻¹)	n	Hf (±2s) (ng g⁻¹)	n	$^{176}Lu/^{177}Hf$ (±2s)	n	$^{176}Hf/^{177}Hf$ (±2s)	n	Digestion method	Instrument	Reference
OKUM	148		551								Certified values (IAG)
	148(5)	12	537(33)	12					Bench-top (150 °C for > 240 h, HF+HNO₃)	ICP-MS	Waterton et al. (2016)
	147(2)	2	585(42)	2					Open vessel multi-acid digestion	ICP-MS	Locmelis et al. (2016)
	138(10)	6	480(66)	6					Pressed powder pellets	LA-ICP-MS	Peters and Pettke 2017)
	130(8)	6	463(58)	6					Pressed powder pellets	LA-ICP-MS	Gilio et al. (2019)
	144(5)	4	514(17)	4	0.0399(07)	4	0.283273(40)	6	Bench-top (100–120 °C for one week)	ID-MC-ICP-MS	This study
	149(2)	5	564(19)	5	0.0375(08)	5	0.283153(23)	5	Bomb (190–200 °C for one week)	ID-MC-ICP-MS	This study
WPR-1	71.6	1	579	1					Bomb (190 °C for five days, HF+HNO₃+HClO₄)	ICP-MS	Chu et al. (2009)
	63.6(1.7)	7	506(26)	7	0.0179(10)	7	0.282979(18)	9	Bench-top (100–120 °C for one week, HF+HNO₃+HClO₄)	ID-MC-ICP-MS	This study
	62.6(1.2)	5	532(20)	5	0.0167(08)	5	0.282960(18)	6	Bomb (190–200 °C for one week, HF+HNO₃+HClO₄)	ID-MC-ICP-MS	This study
NIM-N	104(2)	3	380(30)	3					DAS acid digestion system (180 °C for 16 h under pressure, HF+ HClO₄)	ICP-MS	Dulski (2001)
							0.282824(110)	10	Bomb (190 °C for five days, HF+HNO₃+HClO₄)	MC-ICP-MS	Fourny et al. (2016)
	102(1)	3	356(22)	3	0.0408(25)	3	0.282825(111)	5	Bench-top (100–120 °C for one week, HF+HNO₃+HClO₄)	ID-MC-ICP-MS	This study
	104(1)	8	349(7)	8	0.0423(07)	8	0.282903(21)	11	Bomb (190–200 °C for one week, HF+HNO₃+HClO₄)	ID-MC-ICP-MS	This study
NIM-P	66.6(9)	4	379.6(190)	4					Lithium metaborate fusion	ICP-MS	Hughes et al. (2015, 2016)
							0.282484(72)	3	Bomb (190 °C for five days, HF+HNO₃+HClO₄)	MC-ICP-MS	Fourny et al. (2016)
	63.8(0.5)	4	266(44)	4	0.0343(53)	4	0.282633(240)	6	Bench-top (100–120 °C for one week, HF+HNO₃+HClO₄)	ID-MC-ICP-MS	This study
	64(0.16)	8	281(38)	8	0.0325(39)	8	0.282564(167)	11	Bomb (190–200 °C for one week, HF+HNO₃+HClO₄)	ID-MC-ICP-MS	This study
UB-N	49.3(0.8)	2	115(14)	2					-	ICP-MS	Deschamps et al. (2010)
	45.5(1.4)	6	130(15)	6					Bench-top and bomb (> five days, HF+HNO₃)	ICP-MS	Chauvel et al. (2011)
	49.6(3.4)	12	124(18)	12					Bomb (for five days in par bombs)	ICP-MS	Debret et al. (2019)
	41(8)	6	107(20)	6					Pressed powder pellets	LA-ICP-MS	Peters and Pettke (2017)
	45.0(2.8)	5	145(35)	5					Bench-top (130–140 °C for 36 hours, HF+ HClO₄)	ICP-MS	Rospabé et al. (2018)
	45.5(0.4)	3	125.5(3.0)	3	0.0516(08)	3	0.283245(11)	3	Bench-top (100–120 °C for one week, HF+HNO₃+HClO₄)	ID-MC-ICP-MS	Ma et al. (2019)
	44.2(0.7)	4	126(2)	4	0.0499(16)	4	0.283256(29)	7	Bench-top (100–120 °C for one week, HF+HNO₃+HClO₄)	ID-MC-ICP-MS	This study
	45.7(0.7)	6	125(10)	6	0.0518(40)	6	0.283273(51)	6	Bomb (190–200 °C for one week, HF+HNO₃+HClO₄)	ID-MC-ICP-MS	This study
JP-1	4.0(0.6)	3	127(6)	3					DAS acid digestion system (180 °C for 16 h under pressure, HF+ HClO₄)	ICP-MS	Dulski (2001)
			121(26)	6					Bomb (205 °C for 24 h, HF)	ICP-MS	Tanaka et al. (2003)
	3.966 (0.056)	5	118(4)	5					Bench-top (130 °C for 60 h, HF+HNO₃)	ICP-MS	Babechuk et al. (2010)
	3.944 (0.410)	2	121(1)	2					Bomb (190 °C for 60 h, HF+HNO₃)	ICP-MS	Babechuk et al. (2010)
	4.23 (0.10)	2	113(4)	2					/	ICP-MS	Deschamps et al. (2010)

GEOSTANDARDS and GEOANALYTICAL RESEARCH

Table 3 (continued).

Comparison of Lu and Hf mass fractions, and $^{176}Hf/^{177}Hf$ isotope ratios obtained in this study with published values for mafic-ultramafic rock RMs

RM	Lu (±2s) (ng g⁻¹)	n	Hf (±2s) (ng g⁻¹)	n	$^{176}Lu/^{177}Hf$ (±2s)	n	$^{176}Hf/^{177}Hf$ (±2s)	n	Digestion method	Instrument	Reference
							0.282310(13)	3	Bomb (205 °C for 15 h, HF)	ID-MC-ICP-MS	Lu *et al.* (2007)
			124(10)	5			0.282297(24)	5	Bomb (205 °C for 15 h, HF)	ID-MC-ICP-MS	Lu *et al.* (2007)
	3.93 (0.15)	3	116(3)	3			0.282309(26)	3	Bomb (245 °C for 15 hours, HF)	ID-MC-ICP-MS	Makishima and Nakamura (2008)
	4.05 (0.09)	3	119.1(2.5)	3	0.00483(05)	3	0.282308(11)	3	Bench-top (100–120 °C for one week, HF+HNO₃+HClO₄)	MC-ICP-MS	Ma *et al.* (2019)
	3.99 (0.16)	7	118(4)	7	0.00482(19)	7	0.282301(23)	10	Bench-top (100–120 °C for one week, HF+HNO₃+HClO₄)	ID-MC-ICP-MS	This study
	4.11 (0.34)	2	119(1)	2	0.00492(35)	2	0.282323(17)	4	Bomb (190–200 °C for one week, HF+HNO₃+HClO₄)	ID-MC-ICP-MS	This study
NIM-D	8.58 (0.28)	3	56.9(0.5)	3	0.0214(06)	3	0.282726(20)	3	Bench-top (100–120 °C for one week, HF+HNO₃+HClO₄)	ID-MC-ICP-MS	Ma *et al.* (2019)
	8.51 (0.65)	3	56.5(1.2)	3	0.0214(20)	3	0.282746(36)	4	Bench-top (100–120 °C for one week, HF+HNO₃+HClO₄)	ID-MC-ICP-MS	This study
	7.95 (1.27)	4	53.6(10.9)	4	0.0211(22)	4	0.282727(61)	5	Bomb (190–200 °C for one week, HF+HNO₃+HClO₄)	ID-MC-ICP-MS	This study
MUH-1	19.1		44								Certified values (IAG)
	16(4)	6	32(10)	6					Pressed powder pellets	LA-ICP-MS	Peters and Pettke (2017)
	17(3)	6	36(10)	6					Pressed powder pellets	LA-ICP-MS	Gilio *et al.* (2019)
	18.6(0.8)	3	39(8)	3					Bomb (210 °C for 20 h, HF+HNO₃)	ICP-MS	Ilyinichna *et al.* (2020)
	18.0(0.3)	3	28.6(1.2)	3	0.0895(24)	3	0.28357(20)	3	Bench-top (100–120 °C for one week, HF+HNO₃+HClO₄)	ID-MC-ICP-MS	Ma *et al.* (2019)
	17.9(1.3)	4	27.7(2.9)	4	0.0919(125)	4	0.28361(91)	5	Bench-top (100–120 °C for one week, HF+HNO₃+HClO₄)	ID-MC-ICP-MS	This study
	18.0(0.9)	4	39.8(12.2)	4	0.0655(234)	4	0.283399(206)	5	Bomb (190–200 °C for one week, HF+HNO₃+HClO₄)	ID-MC-ICP-MS	This study
HARZ01	3.08 (0.14)	3	14.2(0.6)	3	0.0307(15)	3	0.282336(19)	3	Bench-top (100–120 °C for one week, HF+HNO₃+HClO₄)	ID-MC-ICP-MS	Ma *et al.* (2019)
	3.05 (0.04)	3	14.6(2.0)	3	0.0297(35)	3	0.282365(24)	4	Bench-top (100–120 °C for one week, HF+HNO₃+HClO₄)	ID-MC-ICP-MS	This study
	2.82 (0.11)	4	14.4(3.1)	4	0.0281(64)	4	0.282376(63)	5	Bomb (190–200 °C for one week, HF+HNO₃+HClO₄)	ID-MC-ICP-MS	This study
DTS-2b	2.01	1	5.55	1					Bomb (140 °C for five days, HF+HClO₄)	ICP-MS	Robin-Popieul *et al.* (2012)
	2.0	1	5.6	1					Bomb (for four days in Parr bomb, HF+HCl)	ICP-MS	Debret *et al.* (2019)
			4.1(0.28)	7					Bench-top (180 °C for four days, HF+ HNO₃)	ID-MC-ICP-MS	Budde *et al.* (2015)
	2.17 (0.03)	3	4.44(0.14)	3	0.0695(13)	3	0.283083(25)	3	Bench-top (100–120 °C for one week, HF+HNO₃+HClO₄)	ID-MC-ICP-MS	Ma *et al.* (2019)
	1.93 (0.45)	3	4.18(0.74)	3	0.0657(90)	3	0.283091(06)	4	Bench-top (100–120 °C for one week, HF+HNO₃+HClO₄)	ID-MC-ICP-MS	This study
	2.08 (0.10)	3	4.48(0.17)	3	0.0657(24)	3	0.283068(29)	5	Bomb (190–200 °C for one week, HF+HNO₃+HClO₄)	ID-MC-ICP-MS	This study

n, number of measurements.

±2s Two standard deviations (intermediate precision) based on *n* measurements and are reported as times 10⁶ for $^{176}Hf/^{177}Hf$ ratios and 10⁴ for $^{176}Lu/^{177}Hf$, except 10⁵ for $^{176}Lu/^{177}Hf$ of JP-1.

For JP-1, several Lu and Hf mass fractions and $^{176}Hf/^{177}Hf$ isotopic data have been previously reported in different studies (Table 3). Lu *et al.* (2009) used ^{179}Hf spike to simultaneously determine the Hf mass fraction and $^{176}Hf/^{177}Hf$ ratio of JP-1 on the Neptune MC-ICP-MS and reported a Hf mass fraction of 124 ± 10 ng g⁻¹, $^{176}Hf/^{177}Hf$ ratio of 0.282297 ± 0.000024 (spiked, 2s, *n* = 5) and 0.282310 ± 0.000013 (non-spiked, 2s, *n* = 3).

Makishima and Nakamura (2008) employed a coprecipitation with Ti compounds to preconcentrate Hf to obtain Lu–Hf data for JP-1 by Neptune MC-ICP-MS. The yielded Lu and Hf mass fractions were 3.93 ± 0.15 ng g⁻¹ (2s, *n* = 3) and 116 ± 3 ng g⁻¹ (2s, *n* = 3), respectively. The corresponding mean $^{176}Hf/^{177}Hf$ ratio was 0.282309 ± 0.000026 (2s, *n* = 3). In this study, using bomb and bench-top digestion, the obtained mean Lu and Hf mass

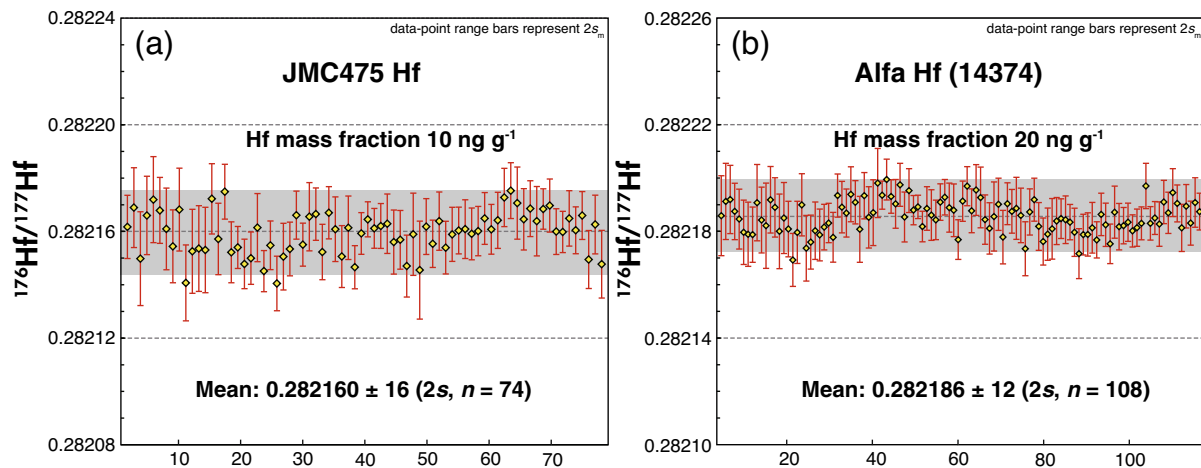**Figure 1.** Long-term ^{176}Hf/^{177}Hf measurement results of (a) JMC475 Hf and (b) Alfa Hf isotope standard solutions (grey bars indicate the intermediate precision expressed at 95% confidence, 2s).

fractions (Lu = 4.02 ± 0.21 ng g^{-1}, Hf = 118 ± 3 ng g^{-1}) were in excellent agreement with previous values on ICP-MS (Dulski 2001, Tanaka *et al.* 2003, Babechuk *et al.* 2010, Deschamps *et al.* 2010). Besides, the ^{176}Lu/^{177}Hf and ^{176}Hf/^{177}Hf isotopic ratios (^{176}Lu/^{177}Hf = 0.00484 ± 0.00021, ^{176}Hf/^{177}Hf = 0.282306 ± 0.000022, 2s, n = 9) in this study show excellent agreement with the results from other laboratories (Lu *et al.* 2007, Makishima and Nakamura 2008).

Ultramafic rock RMs with an Hf mass fraction of 5–100 ng g^{-1}

The Lu and Hf mass fractions and ^{176}Hf/^{177}Hf isotopic data of the ultramafic rock RMs with Hf mass fractions between 5–100 ng g^{-1} are shown in Table 2 and Figure 3. The RMs NIM-D, HAZR01 and DTS-2b showed small intermediate precision for the Lu and Hf mass fractions and Hf isotopic composition. The intermediate precision for ^{176}Hf/^{177}Hf ratios based on independent digestions was better than 60 ppm (2s).

Using the two dissolution methods, the mean value of Lu and Hf mass fractions for NIM-D was 8.19 ± 1.14 ng g^{-1} (2s, n = 7) and 54.9 ± 8.3 ng g^{-1} (2s, n = 7), respectively. The mean ^{176}Lu/^{177}Hf ratio was 0.0212 ± 0.0020 (2s, n = 7) and all ^{176}Hf/^{177}Hf isotopic ratios (spike and non-spiked) yielded a calculated mean of ^{176}Hf/^{177}Hf = 0.282730 ± 0.000054 (2s, n = 9).

For HARZ01, the mean Lu and Hf mass fraction using the two dissolution methods were 2.82 ± 0.26 ng g^{-1} and

14.5 ± 2.5 ng g^{-1} (2s, n = 7), respectively. The corresponding mean ^{176}Lu/^{177}Hf ratio was 0.0288 ± 0.0053 (2s, n = 7), and all ^{176}Hf/^{177}Hf isotopic ratios (spiked and non-spiked) were identical within error ranges with a calculated mean of ^{176}Hf/^{177}Hf = 0.282368 ± 0.000044 (2s, n = 9) and were consistent with our previous obtained values (Ma *et al.* 2019).

The DTS-2b has the lowest Hf mass fraction among the ultramafic rock RMs measured in this study. The Lu mass fractions obtained in this study (2.01 ± 0.17 ng g^{-1}, 2s, n = 6) were in excellent agreement with previously determined values (Robin-Popieul *et al.* 2012, Debret *et al.* 2019; Table 3). The Hf mass fraction agreed well with previous data measured by ID-MC-ICP-MS from Budde *et al.* (2015). The obtained ^{176}Lu/^{177}Hf ratio and ^{176}Hf/^{177}Hf isotope of DTS-2b were 0.0657 ± 0.0059 (2s, n = 6) and 0.283081 ± 0.000026 (2s, n = 6), respectively. The repeatability precision of a single measurement result was better than 65 ppm (2SE).

The serpentinised harzburgite MUH-1 analyses showed reproducible Lu mass fractions but variable Hf mass fractions and ^{176}Hf/^{177}Hf isotopic ratios. In this work, ^{176}Hf/^{177}Hf ratios obtained using bench-top dissolution (^{176}Hf/^{177}Hf = 0.283610 ± 0.000090, 2s, n = 5) were identical within intermediate precision with our previously reported Hf isotope data (^{176}Hf/^{177}Hf = 0.283570 ± 0.000020, 2s, n = 3; Ma *et al.* 2019). Using two dissolution methods, the mean Lu mass fraction was 17.9 ± 1.0 (2s, n = 8), and the Hf mass fractions ranged from 26.5 ng g^{-1} to 46.6 ng g^{-1}, and the ^{176}Lu/^{177}Hf ratios laid within the interval from 0.0527 to 0.1003, the ^{176}Hf/^{177}Hf ratios
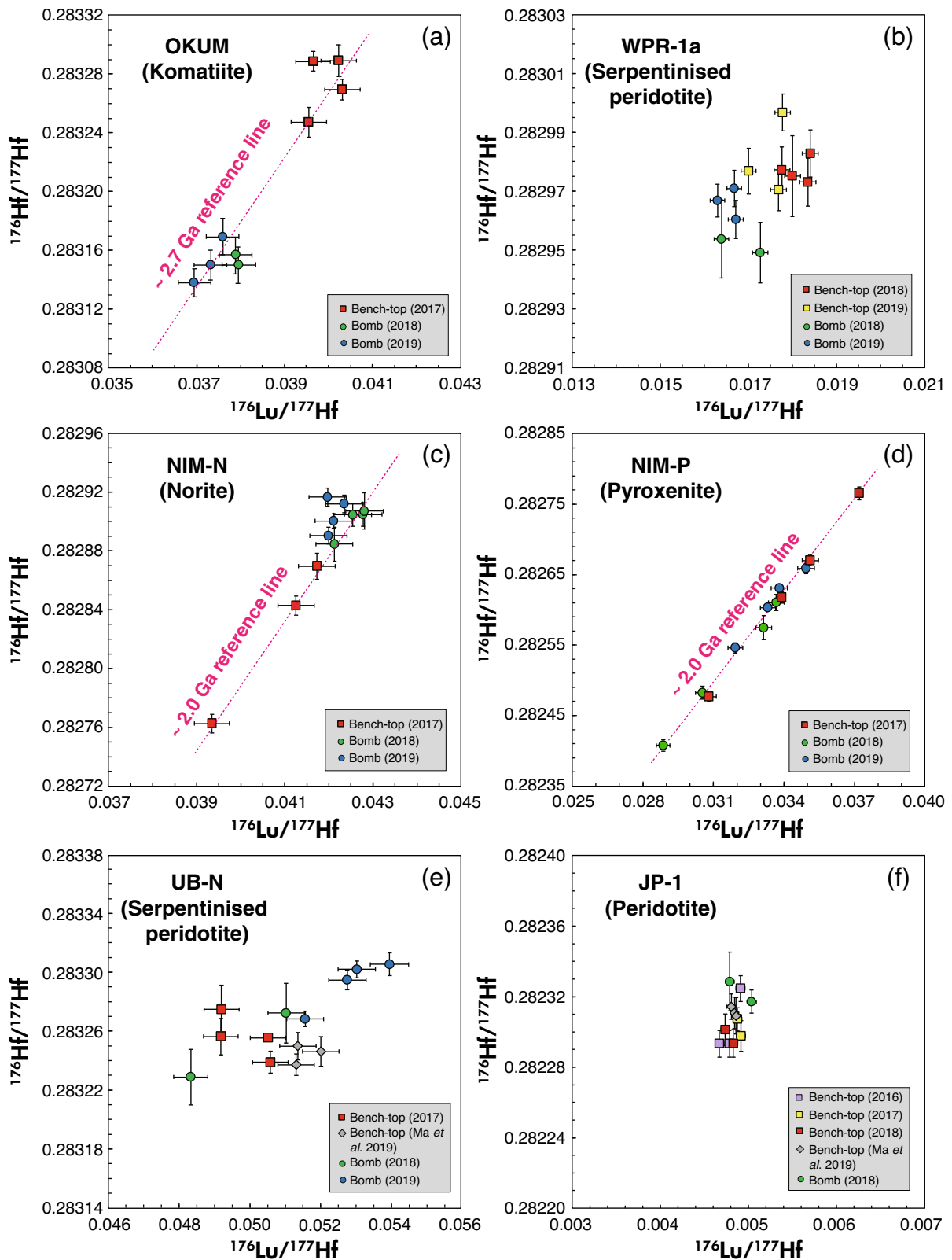
Figure 2. Plots of the Lu–Hf isotopic data from mafic-ultramafic rock RMs with Hf mass fraction of 100–500 ng g⁻¹. Note: "Bench-top" denotes digestion using a Savillex PFA beaker on a hot plate at 100–120 °C; "Bomb" denotes digestion using a high-temperature stainless steel-jacketed PTFE bomb at 190–200 °C.
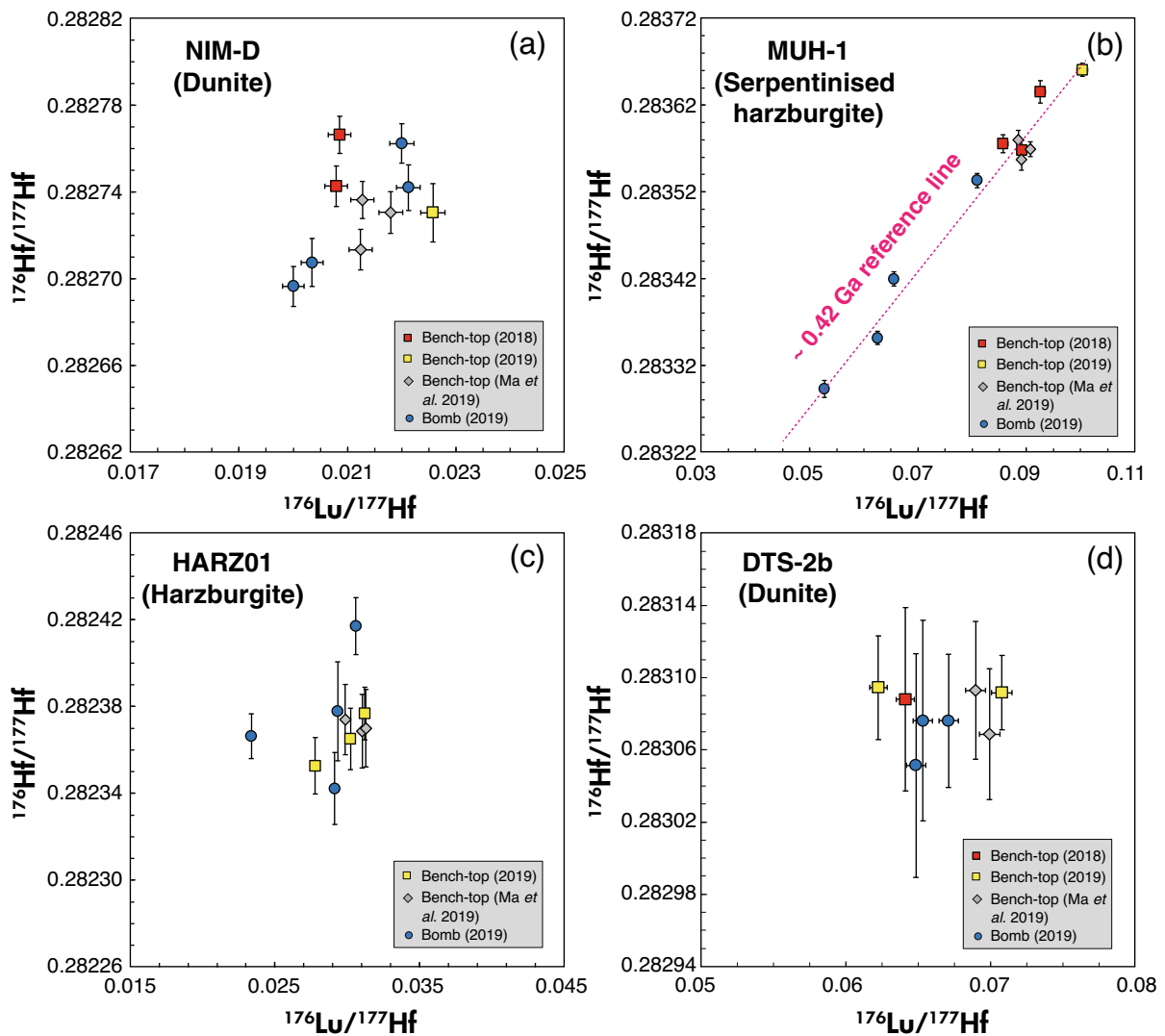
Figure 3. Plots of the Lu–Hf isotopic data from ultramafic rock RMs with Hf mass fraction of 5–100 ng g^{-1}.

ranged from 0.283293 to 0.283661. The Lu and Hf mass fractions were in agreement with previous data within reported precision intervals (Peters and Pettke 2017, Gilio *et al.* 2019, Ilyinichna *et al.* 2020; Table 3).

Comparing bench-top digestion and bomb digestion

Bench-top HF/HNO$_3$ digestion in Savillex PFA beakers on a hot plate (100–120 °C) is effective for basaltic samples; however, it is not adequate for the total dissolution of some rock matrixes when refractory minerals are present, such as garnet, spinel, zircon and chromite (Ionov *et al.* 1992, Yu *et al.* 2001, Meisel *et al.* 2022). Bomb digestion at high temperature (190–200 °C) and extended dissolution time is a useful technique able to decompose

some refractory minerals, such as zircon in rock powder (Meisel *et al.* 2003, Cotta and Enzweiler 2012, Ilyinichna *et al.* 2020). In this study, we evaluate the consistency between two dissolution methods by comparing the mean values and intermediate precision of measurement results for mafic-ultramafic rock RMs. The mean values of bench-top digestion, the mean values of bomb digestion, and associated intermediate precision (2*s*) for measured RMs are summarised in Table 3 and Figure 4.

For the peridotitic RMs UB-N, JP-1, NIM-D, HARZ01 and DTS-2b, the two dissolution methods yielded highly consistent Hf mass fractions and ^{176}Hf/^{177}Hf isotopic ratios (Figure 4). Except HARZ01 yielded lower Lu mass fraction with bomb dissolution than bench-top dissolution. The reason for this discrepancy is unknown, possibly because the concentration is too low to be accurately measured. The
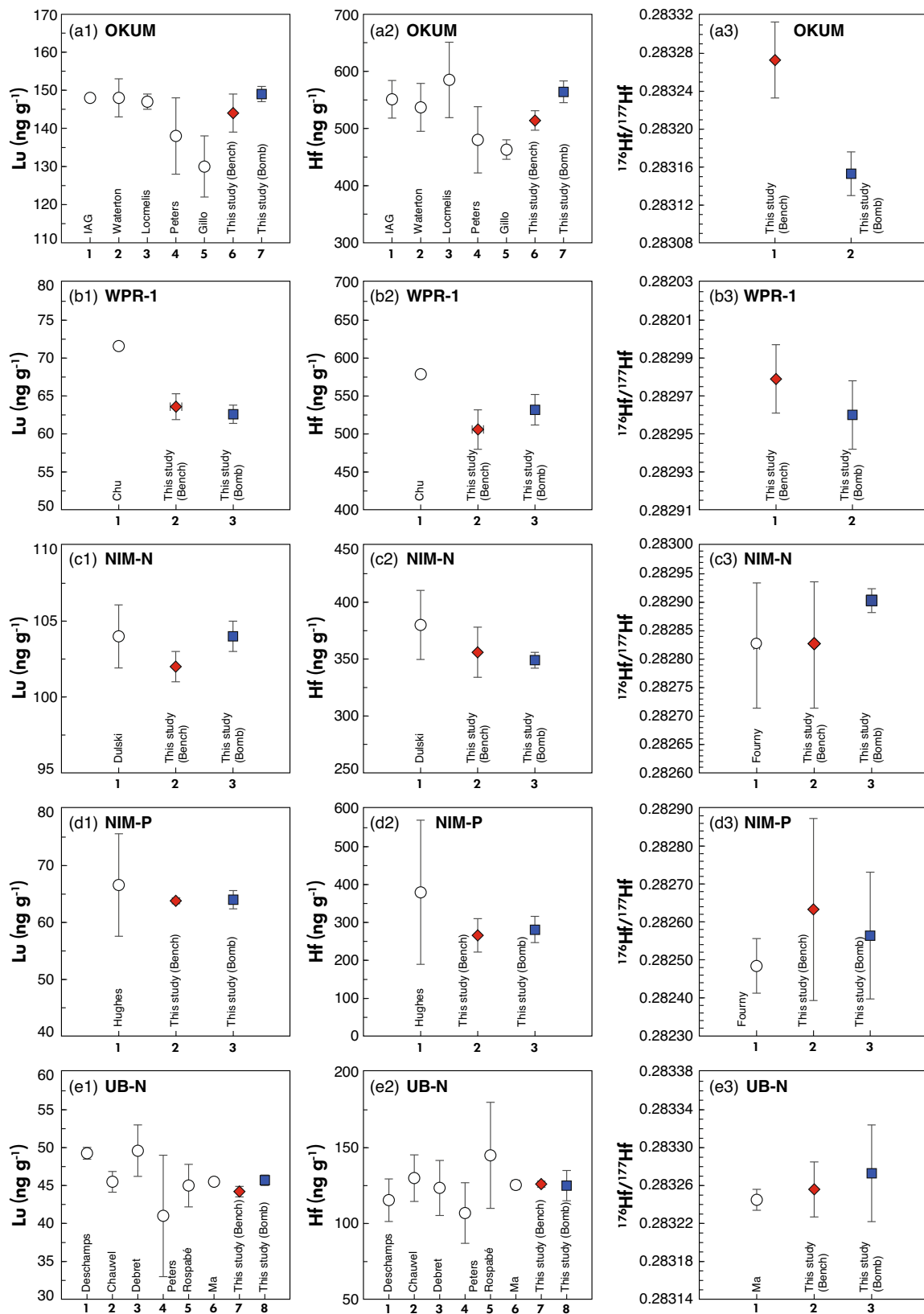
Figure 4. Comparison of Lu, Hf mass fractions and $^{176}Hf/^{177}Hf$ isotopes of ten mafic-ultramafic rock RMs in this study with published values (data from literature are listed in Table 3).
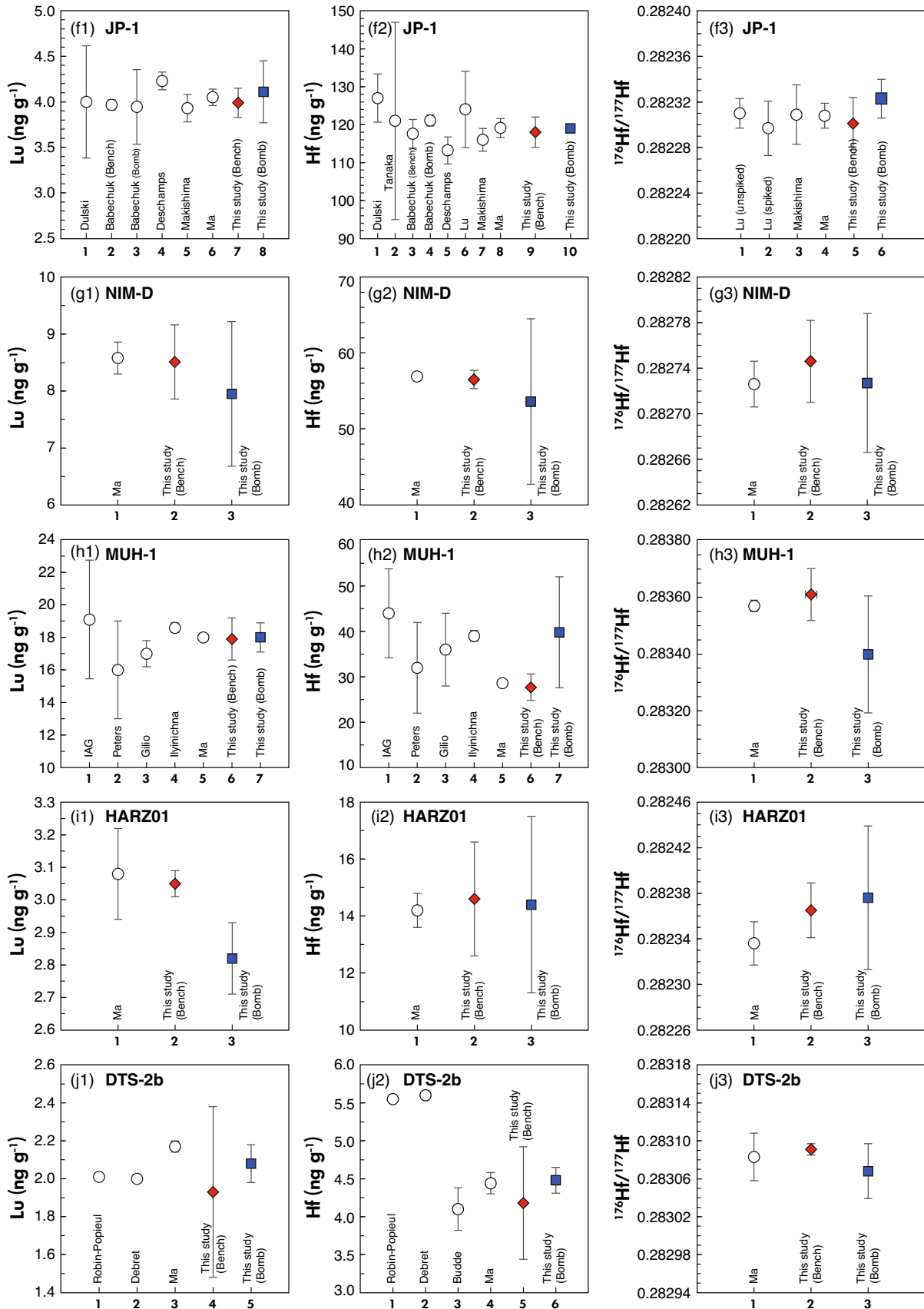
Figure 4. (continued).

^{176}Hf/^{177}Hf ratios for these RMs have intermediate precision better than 60 ppm. In addition, the Lu and Hf mass fractions were within the range of other studies, and the ^{176}Hf/^{177}Hf isotopic values were comparable to those previously published values, indicating that the two methods for dissolving these RMs were both efficient.

However, variable ^{176}Hf/^{177}Hf isotopic ratios between two digestion methods were observed for other mafic-ultramafic RMs in this study. Generally, the bench-top dissolutions were characterised by more radiogenic ^{176}Hf/^{177}Hf isotopic ratios than the bomb dissolutions, which can be attributed to the incomplete dissolution of zircon or other Hf-rich minerals with a non-radiogenic ^{176}Hf/^{177}Hf isotopic ratios in the bench-top dissolution. This is the case for OKUM, WPR-1 and MUH-1. The Lu–Hf data of the OKUM lie on a reference line consistent with a 2.7 Ga age, which is the formation age of the komatiite (Houlé et al. 2009), suggesting that the heterogeneity cannot be explained by contamination during chemistry. The lower Hf mass fraction and systematically higher ^{176}Lu/^{177}Hf ratios in the bench-top-dissolved batch of OKUM indicate that a Hf-rich phase remained undissolved in these samples. The OKUM sample might be able to form zircon as the Zr mass fractions in OKUM were up to 14–19 μg g^{-1}. Besides, chromium spinel (contains several μg g^{-1} Hf) comprises approximately 2–3% of the spinifex-textured komatiite sills in the Serpentine Mountain according to Houlé et al. (2009). Hence, we speculate that both undissolved zircon and spinel might contribute to the poor intermediate precision of the measurement results of Lu-Hf system in OKUM between the two dissolution methods.

For WPR-1, the two dissolution methods yielded consistent Lu mass fractions, whereas the Hf mass fractions with bomb digestion (532 ± 20 ng g^{-1}) were slightly higher than that obtained with bench-top digestion (506 ± 26 ng g^{-1}). The ^{176}Hf/^{177}Hf ratios obtained with bench-top (0.282979 ± 0.000018, 2s, n = 9) were systematically higher than those obtained with bomb digestion (0.282960 ± 0.000006, 2s, n = 9). We attributed this feature to the incomplete dissolution of Hf-rich refractory minerals with non-radiogenic ^{176}Hf/^{177}Hf isotopic ratios. As the Zr mass fractions for WPR-1 was approximately 18–22 μg g^{-1} and spinel is a common accessory mineral in peridotite, we speculate the Hf-rich refractory minerals might be zircon and spinel.

For MUH-1, the Hf mass fractions and ^{176}Hf/^{177}Hf isotopic data obtained after bomb digestion still showed large intermediate precision (2RSD = 31% for Hf mass fractions, 2s = 206 ppm for ^{176}Hf/^{177}Hf value) (Table 2),

whereas the two dissolution methods yielded identical Lu mass fraction. All MUH-1 Lu-Hf data from the two dissolution methods lie on an approximately 0.42 Ga reference line (Figure 3b), which is not odd for the Eastern Alps (Meisel et al. 1997, Melcher and Meisel 2004), suggesting that the heterogeneity cannot be explained by contamination during chemistry. As the Zr mass fraction in MUH-1 was quite low (< 1 μg g^{-1}), it is unlikely to have trace zircons. Hence, we speculate that the Hf-rich refractory minerals might be spinel, which is a common accessory mineral in harzburgite samples. However, as we did not measure residual minerals, this can only be considered a possible interpretation. Garnet (Lu-rich) was not the undissolved phase for WPR-1, OKUM and MUH-1, as the Lu mass fractions with bench-top and bomb dissolutions are not significantly different.

More surprising was the more radiogenic and variable ^{176}Hf/^{177}Hf isotopic ratios in the bomb dissolutions than in the bench-top dissolutions. This was the case for NIM-N; the mean ^{176}Hf/^{177}Hf isotopic ratios in the bomb and bench-top dissolutions were 0.282903 ± 0.000021 (2s, n = 11) and 0.282825 ± 0.000111 (2s, n = 5), respectively. The heterogeneous ^{176}Hf/^{177}Hf isotopic ratios have already been noted in other studies (^{176}Hf/^{177}Hf = 0.282824 ± 0.000110, 2s, n = 10; Fourny et al. 2016). The mean Hf mass fractions of NIM-N measured by bench-top was 356 ± 22 ng g^{-1} (2s, n = 3), more scattered and higher than that measured by the bomb dissolution method (349 ± 7 ng g^{-1}, 2s, n = 8). The Lu mass fractions obtained with the bomb dissolution were identical to those obtained with bench-top dissolution (difference < 2%). This feature cannot be explained by the undissolved zircon with a non-radiogenic Hf in the bomb dissolutions, as this dissolution is proved to be more effective in dissolving zircon than bench-top dissolution. The NIM-P collected from the Bushveld Complex as NIM-N also resulted in poor intermediate precision for the Hf mass fractions (2RSD = 14% for bench-top and 17% for bomb dissolution) and ^{176}Hf/^{177}Hf isotopic ratios (2s = 240 ppm for bench-top and 167 ppm for bomb) (Table 2 and Figure 2c, d). Besides, variable trace element Zr and Hf were previously reported in these RMs (GeoReM online database). The Zr and Hf mass fractions for NIM-N ranged from 9–25.12 μg g^{-1} and 0.18–0.6 μg g^{-1}, respectively. The NIM-P also showed variable Zr and Hf mass fractions, ranging from 7.8–27.4 μg g^{-1} and 0.26–0.48 μg g^{-1}, respectively. The large range in Zr and Hf mass fractions might be the combination of heterogeneity and incomplete digestion. In this study, bomb digestion at 190–200 °C for one week could guarantee complete dissolution of the zircon. Therefore, we suggest that the ^{176}Hf/^{177}Hf isotope variability can be explained by the nugget effect caused by a heterogeneous

distribution of Zr–Hf-rich minerals in each 100 mg test portion. A follow-up study with increasing test portion size is recommended to uncover the exact reason for the isotopic heterogeneity in NIM-P and NIM-N.

In conclusion, the bench-top digestion using Savillex PFA vials is inadequate for the total dissolution of mafic-ultramafic rock samples containing trace Hf-rich refractory minerals (such as zircon, spinel); thus, it is less reliable to acquire accurate Lu-Hf data. We highlight that bomb digestion is essential for the total dissolution of mafic-ultramafic rock for acquiring valid Hf isotopic data, not only for cumulates but for komatiite and peridotitic samples, especially non-zero-aged samples. This conclusion is not novel, as Patchett and co-workers (e.g., Patchett and Tatsumoto 1980, Patchett and Bridgwater 1984, Patchett and Ruiz 1987) among others (Yu *et al.* 2001, Blichert-Toft *et al.* 2004) have insisted on the same for decades. More aggressive digestion methods that work at even higher temperatures and pressure (e.g. HPA-S from Anton Paar) are recommended to yielded complete digestions of refractory minerals and test the homogeneity of these RMs in future studies.

Recommended mafic-ultramafic rocks RMs for Lu–Hf system

The RMs examined in this study may be used for quality control and method validation of Lu and Hf mass fractions and $^{176}Hf/^{177}Hf$ isotopes of unknown mafic-ultramafic rocks. With good intermediate precision (2RSD < 5% for Hf mass fractions of 100–500 ng g^{-1}, < 20% for Hf mass fractions of 5–100 ng g^{-1}; $^{176}Hf/^{177}Hf$ isotopes: 2s < 60 ppm), OKUM, WPR-1, UB-N, JP-1, NIM-D, HARZ01 and DTS-2b are good RMs for data quality control of Lu and Hf mass fractions and $^{176}Hf/^{177}Hf$ isotopes for mafic-ultramafic rock samples. The RMs OKUM, WPR-1, UB-N, and JP-1 can be used to monitor $^{176}Hf/^{177}Hf$ isotopic measurement at low mass fractions (0.1 μg g^{-1} < Hf < 0.5 μg g^{-1}). The RMs NIM-D, HARZ01 and DTS-2b are recommended for Hf isotopic measurement at very low mass fractions (5 ng g^{-1} < Hf < 100 ng g^{-1}). The following values are recommended for the RMs (mean ± 2s) and marked in bold font in Table 2: Lu = 45.1 ± 1.6 ng g^{-1}; Hf = 126 ± 8 ng g^{-1}, $^{176}Lu/^{177}Hf = 0.0510 ± 0.0037$; $^{176}Hf/^{177}Hf = 0.283268 ± 0.000046$; JP-1: Lu = 4.02 ± 0.21 ng g^{-1}; Hf = 118 ± 3 ng g^{-1}, $^{176}Lu/^{177}Hf = 0.00484 ± 0.00021$; $^{176}Hf/^{177}Hf = 0.282306 ± 0.000022$; NIM-D: Lu = 8.19 ± 1.14 ng g^{-1}; Hf = 54.9 ± 8.3 ng g^{-1}, $^{176}Lu/^{177}Hf = 0.0212 ± 0.0020$; $^{176}Hf/^{177}Hf = 0.282730 ± 0.000054$; HARZ01: Lu = 2.82 ± 0.26 ng g^{-1}; Hf = 14.5 ± 2.5 ng g^{-1}, $^{176}Lu/^{177}Hf = 0.0288 ± 0.0053$;

$^{176}Hf/^{177}Hf = 0.282368 ± 0.000044$; DTS-2b: Lu = 2.01 ± 0.17 ng g^{-1}; Hf = 4.33 ± 0.22 ng g^{-1}, $^{176}Lu/^{177}Hf = 0.0657 ± 0.0059$; $^{176}Hf/^{177}Hf = 0.283081 ± 0.000026$. Given the possible Hf-rich refractory minerals, we believe that our values of OKUM (Lu = 149 ± 2 ng g^{-1}; Hf = 564 ± 19 ng g^{-1}, $^{176}Lu/^{177}Hf = 0.0375 ± 0.0008$; $^{176}Hf/^{177}Hf = 0.283153 ± 0.000023$, 2s) and WPR-1 (Lu = 62.6 ± 1.2 ng g^{-1}; Hf = 532 ± 20 ng g^{-1}, $^{176}Lu/^{177}Hf = 0.0167 ± 0.0008$; $^{176}Hf/^{177}Hf = 0.282960 ± 0.000018$, 2s) obtained by high-temperature bomb digestion are more reliable and were selected as reference values. The test portions size for valid mean values and intermediate precision for each RM are listed in Table 2.

The RMs NIM-N, NIM-P, and MUH-1 showed large differences in Lu and Hf mass fractions and Hf isotopes attributed to the heterogeneous powder or incomplete digestion using bomb digestion; thus, these RMs are not recommended to monitor the analysis of Lu–Hf system at 0.1–0.3 test portions.

Conclusions

This study provides Lu and Hf mass fractions, as well as $^{176}Hf/^{177}Hf$ isotopic ratios, of ten commonly used international mafic-ultramafic rock RMs, obtained using the ID-MC-ICP-MS method. The intermediate precision (2s) of Lu and Hf mass fractions and $^{176}Hf/^{177}Hf$ isotopes for RMs OKUM, WPR-1, UB-N, JP-1, NIM-D, HARZ01, and DTS-2b are better than 60 ppm and even good pointing to a homogenous distribution of Lu and Hf bearing minerals at 0.06–0.3 g test portions, and thus, we suggest that these RMs can be used as matrix-matched RMs for data quality control and method validation for low Lu and Hf mass fractions and $^{176}Hf/^{177}Hf$ isotopes measurement of mafic-ultramafic rocks samples. The poor intermediate precision of the Hf mass fraction and $^{176}Hf/^{177}Hf$ isotopes of NIM-N, NIM-P, and MUH-1 was believed to result from the varying proportions of Hf-rich minerals (zircon or spinel?) or incomplete dissolution of refractory minerals in the sample powder. These observations highlight the type of difficulty encountered during geochemical analyses of mafic-ultramafic rocks. To obtain the best possible results, we recommend very fine grinding of the mafic-ultramafic rocks to minimise the nugget effect. Furthermore, we suggest that using the bomb digestion method with extended dissolution time is essential for the total dissolution of mafic-ultramafic rock and acquiring valid Lu and Hf mass fractions and $^{176}Hf/^{177}Hf$ isotopic data, not only for cumulates but also for komatiite and some peridotitic samples, especially non-zero-aged samples.

Our geochemical data contribute to a better characterisation of Lu–Hf systems for the mafic to ultramafic RMs. These new data can be useful for the geochemical community when comparing data from different laboratories.

Acknowledgements

Data availability statement

None.

References

Anguelova M., Fehr M.A., Takazawa E. and Schönbächler M. (2022)
Titanium isotope heterogeneity in the Earth's mantle: A case study of the Horoman peridotite massif. Geochimica et Cosmochimica Acta, 335, 356–368.

Babechuk M.G., Kamber B.S., Greig A., Canil D. and Kodolányi J. (2010)
The behaviour of tungsten during mantle melting revisited with implications for planetary differentiation time scales. Geochimica et Cosmochimica Acta, 74, 1448–1470.

Barfod G.H., Krogstad E.J., Frei R. and Albarède F. (2005)
Lu-Hf and PbSL geochronology of apatites from Proterozoic terranes: A first look at Lu-Hf isotopic closure in metamorphic apatite. Geochimica et Cosmochimica Acta, 69, 1847–1859.

Barnes S.J., Maier W.G. and Curl E.A. (2010)
Composition of the marginal rocks and sills of the Rustenburg Layered Suite, Bushveld Complex, South Africa: Implications for the formation of the platinum-group element deposits. Economic Geology, 105, 1491–1511.

Bast R., Scherer E.E., Sprung P., Fischer-Gödde M., Stracke A. and Mezger K. (2015)
A rapid and efficient ion-exchange chromatography for Lu–Hf, Sm–Nd, and Rb–Sr geochronology and the routine isotope analysis of sub-ng amounts of Hf by MC-ICP-MS. Journal of Analytical Atomic Spectrometry, 30, 2323–2333.

Bizzarro M., Baker J.A. and Ulfbeck D. (2003)
A new digestion and chemical separation technique for rapid and highly reproducible determination of Lu/Hf and Hf isotope ratios in geological materials by MC-ICP-MS. Geostandards Newsletter: The Journal of Geostandards and Geoanalysis, 27, 133–145.

Bizimis M., Griselin M., Lassiter J.C., Salters V.J.M. and Sen G. (2007)
Ancient recycled mantle lithosphere in the Hawaiian plume: Osmium-Hafnium isotopic evidence from peridotite mantle xenoliths. Earth and Planetary Science Letters, 2557, 259–273.

Blichert-Toft J. and Albarède F. (1997a)
The Lu–Hf isotope geochemistry of chondrites and the evolution of the mantle-crust system. Earth and Planetary Science Letters, 148, 243–258.

Blichert-Toft J., Chauvel C. and Albarède F. (1997b)
Separation of Hf and Lu for high-precision isotope analysis of rock samples by magnetic sector-multiple collector ICP-MS. Contributions to Mineralogy and Petrology, 127, 248–260.

Blichert-Toft J. and Arndt N.T. (1999)
Hf isotope compositions of komatiites. Earth and Planetary Science Letters, 171, 439–451.

Blichert-Toft J. (2001)
On the Lu-Hf isotope geochemistry of silicate rocks. Geostandards Newsletter: The Journal of Geostandards and Geoanalysis, 25, 41–56.

Blichert-Toft J., Arndt N.T. and Gruau G. (2004)
Hf isotopic measurements on Barberton komatiites: effects of incomplete sample dissolution and importance for primary and secondary magmatic signatures. Chemical Geology, 207, 261–27.

Bouvier A., Blichert-Toft J., Boyet M. and Albarède F. (2015)
^{147}Sm-^{143}Nd and ^{176}Lu-^{176}Hf systematics of eucrite and angrite meteorites. Meteoritics and Planetary Science, 50, 1896–1911.

Budde G., Kruijer T.S., Fischer-Gödde M., Irving A.J. and Kleine T. (2015)
Planetesimal differentiation revealed by the Hf–W systematics of ureilites. Earth and Planetary Science Letters, 430, 316–325.

Chu Z.Y., Wu F.Y., Walker R.J., Rudnick R.L., Pitcher L., Puchtel I.S. and Wilde S.A. (2009)
Temporal evolution of the lithospheric mantle beneath the eastern North China Craton. Journal of Petrology, 50, 1857–1898.

Chu Z.Y., Guo J.H., Yang Y.H., Qi L. and Li C.F. (2014)
Precise determination of Sm and Nd concentrations and Nd isotopic compositions in highly depleted ultramafic reference materials. Geostandards and Geoanalytical Research, 24, 1534–1544.

Chauvel C., Bureau S. and Poggi C. (2011)
Comprehensive chemical and isotopic analyses of basalt and sediment reference materials. Geostandards and Geoanalytical Research, 35, 125–143.

references

Connelly J.N., Ulfbeck D.G., Thrane K., Bizzarro M. and Housh T. (2006)
A method for purifying Lu and Hf for analyses by MC-ICP-MS using TODGA resin. Chemical Geology, 233, 126–136.

Cotta A.J.B. and Enzweiler J. (2011)
Classical and new procedures of whole rock dissolution for trace element determination by ICP-MS. Geostandards and Geoanalytical Research, 36, 27–50.

Debret B., Albers E., Walter B., Price R., Barnes J.D., Beunon H. and Williams H. (2018)
Shallow forearc mantle dynamics and geochemistry: New insights from the IODP expedition 366. Lithos, 326–327, 230–245.

Deschamps F., Guillot S., Godard M., Chauvel C., Andreani M. and Hattori K. (2010)
In situ characterization of serpentinites from forearc mantle wedges: Timing of serpentinization and behavior of fluid-mobile elements in subduction zones. Chemical Geology, 269, 262–277.

Dulski P. (2001)
Reference materials for geochemical studies: New analytical data by ICP-MS and critical discussion of reference values. Geostandards Newsletter: The Journal of Geostandards and Geoanalysis, 25, 87–125.

Fourny A., Weis D. and Scoates J.S. (2016)
Comprehensive Pb-Sr-Nd-Hf isotopic, trace element, and mineralogical characterization of mafic to ultramafic rock reference materials. Geochemistry, Geophysics, Geosystems, 17, 739–773.

Frisby C., Bizimis M. and Mallick S. (2016)
Hf–Nd isotope decoupling in bulk abyssal peridotites due to serpentinization. Chemical Geology, 440, 60–72.

Gilio M., Scambelluri M., Agostini S., Godard M., Peters D. and Pettke T. (2019)
Petrology and geochemistry of serpentinites associated with the ultra-high pressure Lago di Cignana Unit (Italian Western Alps). Journal of Petrology, 60, 1229–1262.

Govindaraju K. (1982)
Report (1967–1981) on four ANRT rock reference samples diorite DR-N, serpentine UB-N, bauxite BX-N and disthene DT-N. Geostandards Newsletter, 6, 91–159.

Halliday A.N., Lee D.C., Christensen J.N., Rehkämper M., Yi W. and Luo X.Z. (1998)
Applications of multiple collector-ICP-MS to cosmochemistry, geochemistry, and paleoceanography. Geochimica et Cosmochimica Acta, 62, 919–940.

Huang K.F., Blusztajn J., Oppo D.W., Curry W.B. and Peucker-Ehrenbrink B. (2012)
High-precision and accurate determinations of neodymium isotopic compositions at nanogram levels in natural materials by MC-ICP-MS. Journal of Analytical Atomic Spectrometry, 27, 1560–1567.

Houlé M.G., Préfontaine S., Fowler A.D. and Gibson H.L. (2009)
Endogenous growth in channelized komatiite lava flows: evidence from spinifex-textured sills at Pyke Hill and Serpentine Mountain, Western Abitibi Greenstone Belt, northeastern Ontario, Canada. Bulletin of Volcanology, 71, 881–901.

Hughes H.S.R., McDonald I. and Kerr A.C. (2015)
Platinum-group element signatures in the North Atlantic Igneous Province: Implications for mantle controls on metal budgets during continental breakup. Lithos, 233, 89–110.

Hughes H.S.R., McDonald I., Faithfull J.W., Upton B.G.J. and Loocke M. (2016)
Cobalt and precious metals in sulphides of peridotite xenoliths and inferences concerning their distribution according to geodynamic environment: A case study from the Scottish lithospheric mantle. Lithos, 240–243, 202–227.

Iizuka T., Yamaguchi T., Itano K., Hibiya Y. and Suzuki K. (2017)
What Hf isotopes in zircon tell us about crust–mantle evolution. Lithos, 274–275, 304–327.

Ilyinichna O.O., Michailovich L.S., Sergeevich D.A. and Gennadievna E.K. (2020)
An investigation of trace elements' behavior during a chemical preparation of ultramafic matrix rock sample using bomb digestion for analysis by ICP-MS. Journal of Analytical Atomic Spectrometry, 35, 2627–2638.

Ionov D.A., Savoyant L. and Dupuy C. (1992)
Application of the ICP-MS technique to trace element analysis of peridotites and their minerals. Geostandards Newsletter, 16, 311–315.

Jain J.C., Field M.P., Neal C.R., Ely J.C. and Sherrell R.M. (2000)
Determination of the REE in geological reference materials DTS-1 (dunite) and PCC-1 (peridotite) by ultrasonic and microconcentric desolvating nebulisation ICP-MS. Geostandards Newsletter: The Journal of Geostandards and Geoanalysis, 24, 65–72.

Jochum K.P. and Nohl U. (2008)
Reference materials in geochemistry and environmental research and the GeoReM database. Chemical Geology, 253, 50–53.

Le Févre B. and Pin C. (2005)
A straightforward separation scheme for concomitant Lu-Hf and Sm-Nd isotope ratio and isotope dilution analysis. Analytica Chimica Acta, 543, 209–221.

Locmelis M., Fiorentini M.L., Rushmer T., Arevalo R., Adam J. and Denyszyn S.W. (2016)
Sulfur and metal fertilization of the lower continental crust. Lithos, 244, 74–93.

references

Li C.F., Guo J.H., Yang Y.H., Chu Z.Y. and Wang X.C. (2014)
Single-step separation scheme and high-precision isotopic ratios analysis of Sr–Nd–Hf in silicate materials. Journal of Analytical Atomic Spectrometry, 29, 1467–1476.

Lu Y.H., Makishima A. and Nakamura E. (2007)
Purification of Hf in silicate materials using extraction chromatographic resin, and its application to precise determination of $^{176}Hf/^{177}Hf$ by MC-ICP-MS with ^{179}Hf spike. Journal of Analytical Atomic Spectrometry, 22, 69–76.

Ma Q., Yang M., Zhao H., Evans N.J., Chu Z.Y., Xie L.W., Huang C., Zhao Z.D. and Yang Y.H. (2019)
Accurate and precise determination of Lu and Hf mass fractions and Hf isotopic composition at the sub-nanogram level in geological samples using MC-ICP-MS. Journal of Analytical Atomic Spectrometry, 34, 1256–1262.

Makishima A. and Nakamura E. (2008)
New preconcentration technique of Zr, Nb, Mo, Hf, Ta and W employing coprecipitation with Ti compounds: Its application to Lu-Hf system and sequential Pb-Sr-Nd-Sm separation. Geochemical Journal, 42, 199–206.

Makishima A. and Nakamura E. (2010)
Precise isotopic determination of Hf and Pb at sub-nano gram levels by MC-ICP-MS employing a newly designed sample cone and a pre-amplifier with a 10^{12} ohm register. Journal of Analytical Atomic Spectrometry, 25, 1712–1716.

Mallick S., Standish J.J. and Bizimis M. (2015)
Constraints on the mantle mineralogy of an ultra-slow ridge: Hafnium isotopes in abyssal peridotites and basalts from the 9–25°E Southwest Indian Ridge. Earth and Planetary Science Letters, 410, 42–53.

Meisel T., Melcher F., Tomascak P., Dingeldey C. and Koller F. (1997)
ReOs isotopes in orogenic peridotite massifs in the Eastern Alps, Austria. Chemical Geology, 143, 217–229.

Meisel T., Reisberg L., Moser J., Carignan J., Melcher F. and Brügmann G. (2003)
Re–Os systematics of UB-N, a serpentinized peridotite reference material. Chemical Geology, 201, 161–179.

Meisel T., Webb P. and Rachetti A. (2022)
Highlights from 25 Years of the GeoPT Programme: What can be learnt for the advancement of geoanalysis. Geostandards and Geoanalytical Research, 46, 223–243.

Melcher F. and Meisel T. (2004)
A metamorphosed early Cambrian crust-mantle transition in the Eastern Alps, Austria. Journal of Petrology, 45, 1689–1723.

Mortensen J.K. and Hulbert L.J. (1991)
A U-Pb zircon age for a Maple Creek gabbro sill, Tatamagouche Creek area, southwest Yukon Territory. Radiogenic Age and Isotopic Studies, Report 5. Geological Survey of Canada, Paper, 91–2, 175–179.

Münker C., Weyer S., Scherer E. and Mezger K. (2001)
Separation of high field strength elements (Nb, Ta, Zr, Hf) and Lu from rock samples for MC-ICP-MS measurements. Geochemistry, Geophysics, Geosystems, 2, 2001GC000183.

Patchett P.J. and Bridgwater D. (1984)
Origin of continental crust of 1.9–1.7 Ga age defined by Nd isotopes in the Ketilidian terrain of South Greenland. Contributions to Mineralogy and Petrology, 87, 311– 318.

Patchett P.J. and Tatsumoto M. (1980)
A routine high-precision method for Lu–Hf isotope geochemistry and chronology. Contributions to Mineralogy and Petrology, 75, 263–267.

Patchett P.J. and Ruiz J. (1987)
Nd isotopic ages of crust formation and metamorphism in the Precambrian of eastern and southern Mexico. Contributions to Mineralogy and Petrology, 96, 523– 528.

Peters D. and Pettke T. (2016)
Evaluation of major to ultra trace element bulk rock chemical analysis of nanoparticulate pressed powder pellets by LA-ICP-MS. Geostandards and Geoanalytical Research, 41, 5–28.

Pin C. and Santos Zalduegui J.F. (1997)
Sequential separation of light rare-earth elements, thorium and uranium by miniaturized extraction chromatography: Application to isotopic analyses of silicate rocks. Analytica Chimica Acta, 339, 79–89.

Ragan D.M. (1963)
Emplacement of the Twin Sisters dunite, Washington. American Journal of Science, 261, 549–565.

Robin-Popieul C.C.M., Arndt N.T., Chauvel C., Byerly G.R., Sobolev A.V. and Wilson A. (2012)
A new model for Barberton komatiites: Deep critical melting with high melt retention. Journal of Petrology, 53, 2191– 2229.

Rospabé M., Benoit M. and Candaudap F. (2017)
Determination of trace element mass fractions in ultramafic rocks by HR-ICP-MS: A Combined approach using a direct digestion/dilution method and preconcentration by coprecipitation. Geostandards and Geoanalytical Research, 42, 115–129.

Salters V.J.M. and Zindler A. (1995)
Extreme $^{176}Hf/^{177}Hf$ in the sub-oceanic mantle. Earth and Planetary Science Letters, 129, 13–30.

Salters V.J.M., Mallick S., Hart S.R., Langmuir C.E. and Stracke A. (2011)
Domains of depleted mantle: New evidence from hafnium and neodymium isotopes. Geochemistry, Geophysics, Geosystems, 12, Q08001.

Scherer E., Münker C. and Mezger K. (2001)
Calibration of the lutetium-hafnium clock. Science, 293, 683–687.

Scoates J.M. and Friedman R.M. (2008)
Precise age of the platiniferous Merensky reef, Bushveld Complex, South Africa, by the U-Pb zircon chemical abrasion ID-TIMS technique. Economic Geology, 203, 465–471.

references

Sun Y.L., Sun S.L., Wang C.Y. and Xu P. (2013)
Determination of rare earth elements and thorium at nanogram levels in ultramafic samples by inductively coupled plasma-mass spectrometry combined with chemical separation and pre-concentration. Geostandards and Geoanalytical Research, 37, 65–76.

Tanaka R., Makishima A., Kitagawa H. and Nakamura E. (2003)
Suppression of Zr, Nb, Hf and Ta coprecipitation in fluoride compounds for determination in Ca-rich materials. Journal of Analytical Atomic Spectrometry, 18, 1458–1463.

Toy V.G., Newman J., Lamb W. and Tikoff B. (2009)
The role of pyroxenites in formation of shear instabilities in the mantle: Evidence from an ultramafic ultramylonite, Twin Sisters Massif, Washington. Journal of Petrology, 51, 55–80.

Vervoort J.D., Patchett P. J., Söderlund U. and Baker M. (2004)
Isotopic composition of Yb and the determination of Lu concentrations and Lu/Hf ratios by isotope dilution using MC-ICP-MS. Geochemistry, Geophysics, Geosystems, 5, Q11002.

Vervoort J.D. and Kemp A.I.S. (2016)
Clarifying the zircon Hf isotope record of crust–mantle evolution. Chemical Geology, 425, 65–75.

Waterton P., Pearson D.G., Kjarsgaard B., Hulbert L., Locock A., Parman S. and Davis B. (2017)
Age, origin, and thermal evolution of the ultra-fresh ~ 1.9 Ga Winnipegosis Komatiites, Manitoba, Canada. Lithos, 268–271, 114–130.

Webb P.C., Thompson M., Potts P.J., Gowing C.J.B., Meisel T.C. (2016)
GeoPT38A – An international proficiency test for analytical geochemistry laboratories – Special report on round 38a (Modified harzburgite, HARZ01). International Association of Geoanalysts: Published report.

Weis D., Kieffer B., Maerschalk C., Pretorius W. and Barling J. (2005)
High-precision Pb-Sr-Nd-Hf isotopic characterization of USGS BHVO-1 and BHVO-2 reference materials. Geochemistry, Geophysics, Geosystems, 6, Q02002.

Weis D., Kieffer B., Hanano D., Nobre Silva I., Barling J., Pretorius W., Maerschalk C. and Mattielli N. (2007)
Hf isotope compositions of U.S. Geological Survey reference materials. Geochemistry, Geophysics, Geosystems, 8, Q06006.

Xiong Q., Griffin W.L., Zheng J.P., O'Reilly S.Y., Pearson N.J., Xu B. and Belousova E.A. (2016)
Southward trench migration at ~ 130–120 Ma caused accretion of the Neo-Tethyan forearc lithosphere in Tibetan ophiolites. Earth and Planetary Science Letters, 438, 57–65.

Yang Y.H., Zhang H.F., Chu Z.Y., Xie L.W. and Wu F.Y. (2010)
Combined chemical separation of Lu, Hf, Rb, Sr, Sm and Nd from a single rock digest and precise and accurate isotope determinations of Lu-Hf, Rb-Sr and Sm-Nd isotope systems using multi-collector ICP-MS and TIMS. International Journal of Mass Spectrometry, 290, 120–126.

Yang M., Yang Y.H., Evans N.J., Xie L.W., Huang C., Wu S.T., Yang J.H. and Wu F.Y. (2020a)
Precise and accurate determination of Lu and Hf contents, and Hf isotopic compositions in Chinese rock reference materials by MC-ICP-MS. Geostandards and Geoanalytical Research, 44, 553–565.

Yang Y.H., Yang M., Jochum K.P., Wu S.T., Zhao H., Xie L.W., Huang C., Zhan X.C., Yang J.H. and Wu F.Y. (2020b)
High-precision Sr-Nd-Hf-Pb isotopic composition of Chinese geological standard glasses CGSG-1, CGSG-2, CGSG-4 and CGSG-5 reference materials by MC-ICP-MS and TIMS. Geostandards and Geoanalytical Research, 44, 567–579.

Yokoyama T., Makishima A. and Nakamura E. (1999)
Evaluation of the coprecipitation of incompatible trace elements with fluoride during silicate rock dissolution by acid digestion. Chemical Geology, 157, 175–187.

Yu Z., Robinson P. and McGoldrick P. (2001)
An evaluation of methods for the chemical decomposition of geological materials for trace element determination using ICP-MS. Geostandards Newsletter: The Journal of Geostandards and Geoanalysis, 25, 199–217.

Yu Z., Robinson P., Townsend A.T., Münker C. and Crawford A.J. (2000)
Determination of high field-strength elements, Rb, Sr, Mo, Sb, Cs, Tl and Bi at ng g^{-1} levels in geological reference materials by magnetic sector ICP-MS after HF/HClO$_4$ high pressure digestion. Geostandards Newsletter: The Journal of Geostandards and Geoanalysis, 24, 39–50.

Zhao X.M., Wang H., Li Z.H., Evans N.J., Ying J.F., Yang Y.H. and Zhang H.F. (2021)
Nature and evolution of lithospheric mantle beneath the western North China Craton: Constraints from peridotite and pyroxenite xenoliths in the Sanyitang basalts. Lithos, 384–385, 105987.